UNCLASSIFIED

AD NUMBER
ADC017575
CLASSIFICATION CHANGES
TO: unclassified
FROM: secret
LIMITATION CHANGES
TO: Approved for public release, distribution unlimited
FROM: Distribution authorized to U.S. Gov't. agencies only; Test and Evaluation; 01 FEB 1979. Other requests shall be referred to Commander, Naval Air Development Center, Warminster, PA 18974.
AUTHORITY
31 Dec 1989, per document marking; CNO/N772 ltr N772A/6U875630, 20 Jan 2006 & ONR ltr 31 Jan 2006

THIS PAGE IS UNCLASSIFIED

SECRET

B.S. 2

AD C017575

LEVEL III

VOLUME II

SELF-TENSIONING ACOUSTICAL
HORIZONTAL LINE ARRAY
(SPRAY)
DATA ANALYSIS (U)

FINAL REPORT OF BEARING STAKE TESTS
JANUARY THRU MARCH 1978

9 JANUARY 1979

DDC FILE COPY

PREPARED FOR

NAVAL AIR DEVELOPMENT CENTER
WARMINSTER, PENNSYLVANIA

UNDER CONTRACTS
N62269-77-C-0139
and
N62269-78-M-6884

PREPARED BY

SANDERS ASSOCIATES, INC.
OCEAN SYSTEMS DIVISION
95 CANAL STREET
NASHUA, NEW HAMPSHIRE 03061

79 04 04 509

SECRET

ACCESSION for
NTIS White Section [ ]
DDC Buff Section [X]
UNANNOUNCED [ ]
JUSTIFICATION
BY
DISTRIBUTION/AVAILABILITY CODES
Dist. AVAIL. and/or SPECIAL
B

SECRET

2

VOLUME II

SELF-TENSIONING ACOUSTICAL HORIZONTAL LINE ARRAY (SPRAY) DATA ANALYSIS. (U)

LEVEL III

FINAL REPORT OF BEARING STAKE TESTS

JANUARY THRU MARCH 1977.

Volume II. Data Analysis Facility and Data Reduction Methodology.

9 JANUARY 1979

NATIONAL SECURITY INFORMATION
UNAUTHORIZED DISCLOSURE SUBJECT TO CRIMINAL SANCTIONS

PREPARED FOR

NAVAL AIR DEVELOPMENT CENTER
WARMINSTER, PENNSYLVANIA 18974

UNDER CONTRACTS

N62269-77-C-0139

and

N62269-78-M-6884

Distribution limited to U.S. Gov't. agencies only; T&E; Proprietary Info.; 1 Feb 1979. Other requests for this document must be referred to

DDC
MAY 10 1979
D

PREPARED BY

SANDERS ASSOCIATES, INC.
OCEAN SYSTEMS DIVISION
95 CANAL STREET
NASHUA, NEW HAMPSHIRE 03061

Classification Reviewed & Approved By

R. L. Townsend 10 Jan 1979
R. L. Townsend Date

CLASSIFIED BY DD 254 1 Dec 76
N62269-77-C-0139
Exempt from GDS of EO 11652
Exemption Category 3
Declassify on 31 Dec 1989

SAI DOCUMENT CONTROL #
1-10-597-2

SECRET

VOLUME	
IA	Summary - Test Results
IB	Detailed Description, Test Results
II	Data Analysis Facility and Data Reduction Methodology
IIIA	Data Points 1, 2 and 3 Raw Data
IIIB	Data Points 4, 5 and 6 Raw Data
IVA	Data Points 7, 8 and 9 Raw Data
IVB	Data Points 10, 11 and 12 Raw Data

TABLE OF CONTENTS

Section I
Introduction

Section II
Data Reduction Hardware

Section III
Data Processing Procedures

TABLE OF CONTENTS (Cont)

Section IV

Measured/Theoretical Performance Evaluation

LIST OF ILLUSTRATIONS

LIST OF TABLES

SECTION 1

(U) INTRODUCTION (U)

(U) This document is Volume 2 of the 4-volume set comprising the final report of the Bearing Stake Sea Tests of January, February, and March, 1977, performed on the Self-Tensioning Acoustic Horizontal Line Array (SPRAY), under Contract N62269-77-C-0139 for the Naval Air Development Center, Warminster, Pennsylvania.

(U) This volume describes the total SPRAY data reduction effort performed on the SPRAY Sea Test Data. There are descriptions included to familiarize the reader with the data processing instrumentation configuration, the instrumentation capabilities and the associated calibration tests and results. Other volumes of the set are referenced, as necessary, when results are discussed.

(U) Also included are detailed explanations for the data reduction and analysis procedures used in generating the operational performance results of the Sanders SPRAY Acoustic Array System.

SECTION 2

(U) DATA REDUCTION HARDWARE (U)

(U) 2.1 INSTRUMENTATION CONFIGURATION (U)

(U) The two signal processing instrumentations used for the reduction of the SPRAY Sea Test Data can be separated into four major subsystems:

- Analog Tape System
- SPRAY Demultiplexer System
- SPRAY Beamformer System
- Digital Signal Processor and Display System

Figure 2-1 and figure 2-2 show the interconnection of these subsystems.

(U) The signal presented to the processing system originated at the analog tape recorder. The tape recorder reproduces the multiplexed composite signal produced by the SPRAY Acoustic Array during the Sea Test operations. The composite signal is cabled to the SPRAY demultiplexor where the 53 channels of acoustic data, the 2 channels of compass data and 2 channels of tension data are recovered for processing. The 53 channels of demultiplexed acoustic data are passed to the digital beamformer where steerable beamforming is accomplished. The beamformer produces up to 4 simultaneous beamformed outputs. These outputs are sent to the Sanders 6108 Digital Signal Processor or the Sanders MCPS-32 Signal Processor for spectral analysis, integration, and output display. The 6108 Digital Signal Processor System can accommodate up to three channels of input and produce either ALIU hard copy outputs or LOFAR-type electrographic recordings. The MCPS-32 Digital Signal Processor System can accept 32 channels of input and produce either ALIU grams on a CRT or X-Y displays of frequency vs amplitude on CRT for operator usage. Signal and noise levels may be obtained from the X-Y displays. A hard copy plot may be obtained of the frequency vs amplitude display utilizing an external plotter. Accurate signal or noise levels cannot be gained from these plots.

(U) The 2 channels of compass data were input to a strip chart recorder and array heading information was obtained.

(U) The 2 channels of tension data was not suitable for processing.

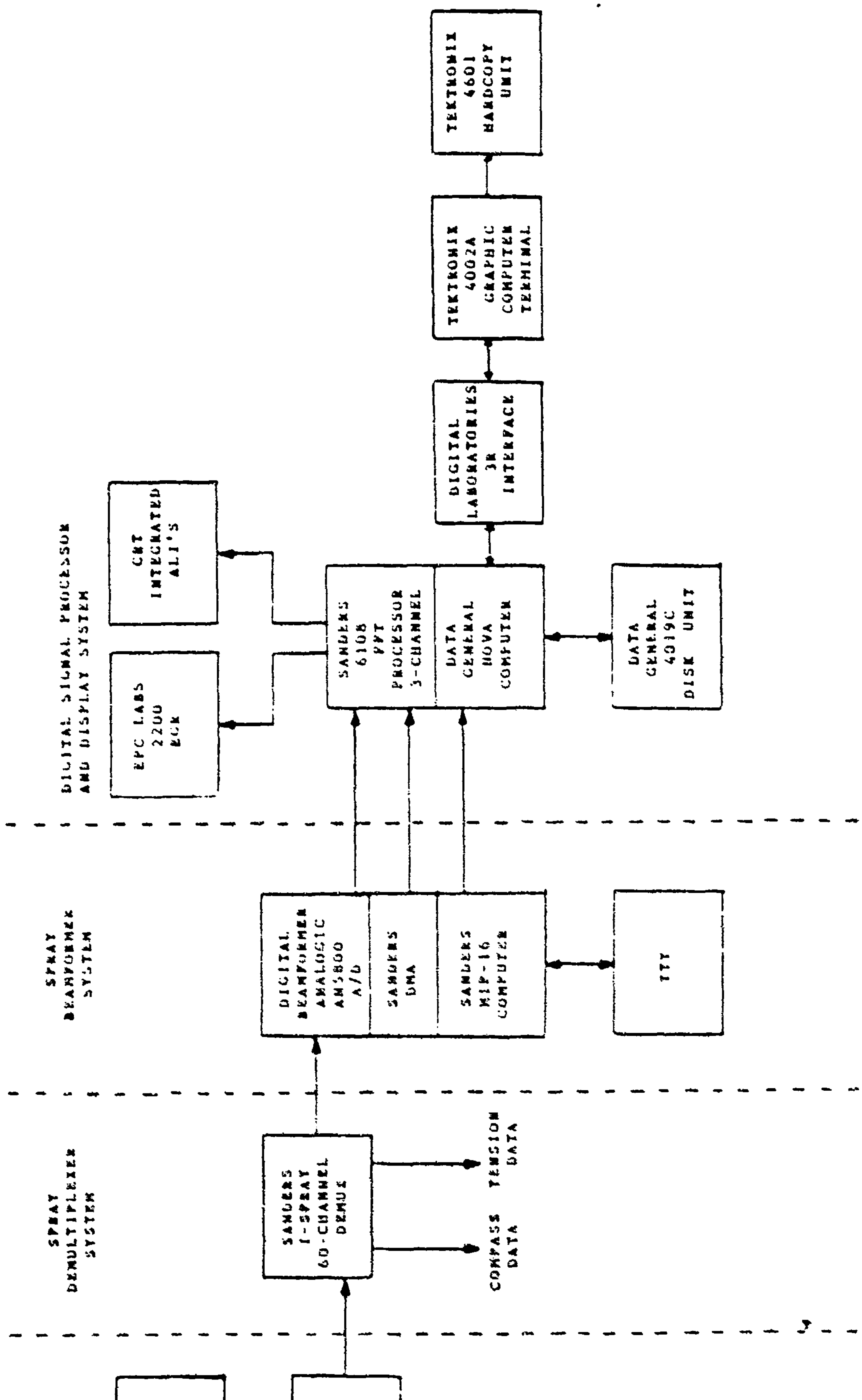

(U) FIGURE 2-1 DATA PROCESSING INSTRUMENTATION BLOCK DIAGRAM (U)

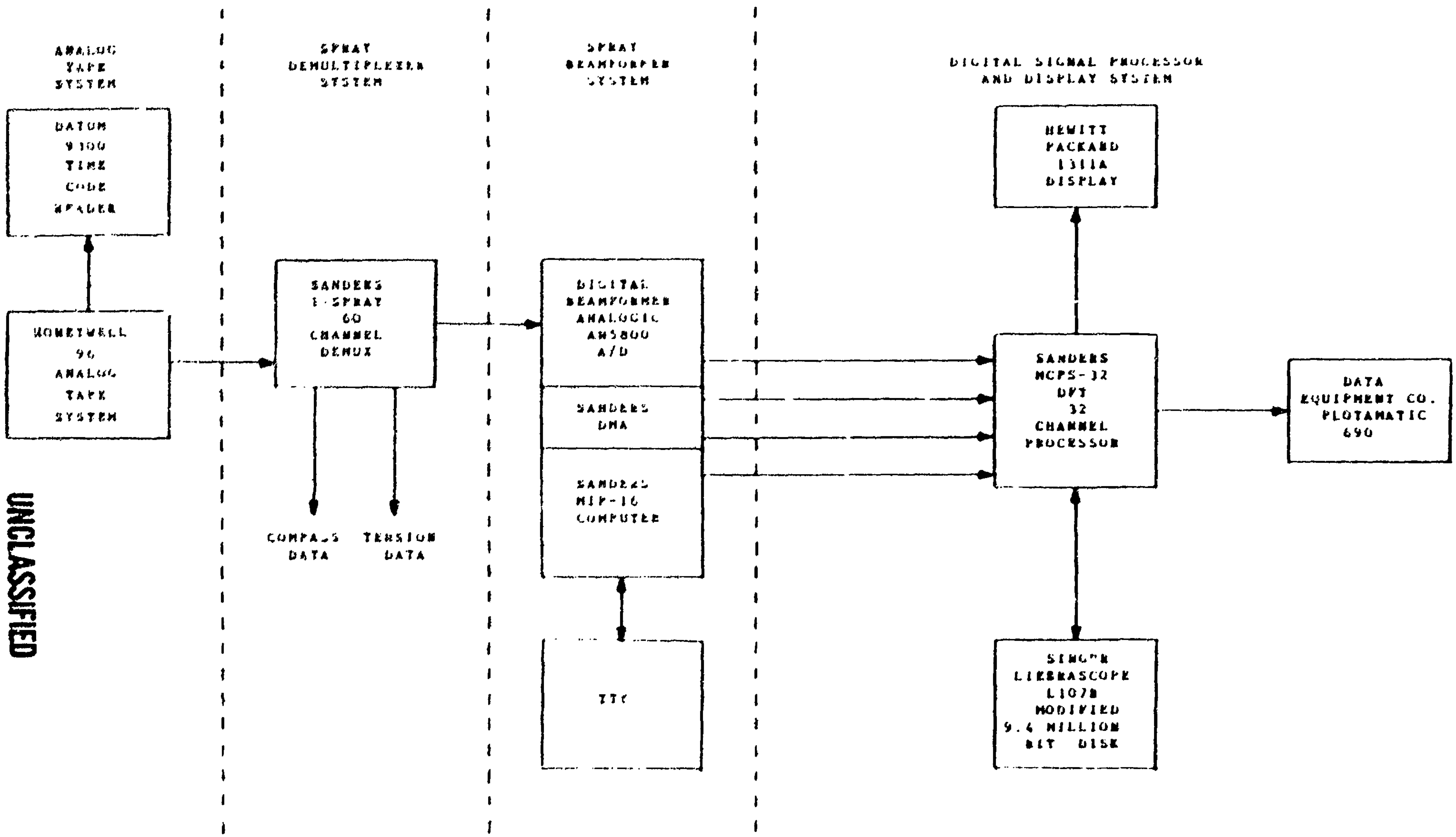

(U) FIGURE 2-2 DATA PROCESSING INSTRUMENTATION BLOCK DIAGRAM (U)

(U) 2.2 HARDWARE DESCRIPTION (U)

(U) The following paragraphs briefly describe each major subsystem of the SPRAY Data Processing Instrumentation.

(U) 2.2.1 ANALOG TAPE SYSTEM (U)

(U) A Honeywell Model 96 Analog Tape System, utilized to reproduce the SPRAY Sea Test Data, was operated in the tape servo mode at 30 IPS (X1 speed) for all data processing runs. In addition to reproducing the SPRAY composite signal for processing, the time code track was reproduced and the resulting IRIGB time code cabled to a time code reader providing accurate event times for each segment of data selected for processing.

(U) 2.2.2 SPRAY DEMULTIPLEXER SYSTEM (U)

(U) The SPRAY Demultiplexer System up-translates and demultiplexes the multiplexer data from the magnetic tape into the original 64 sensor channels for processing. The demultiplexer system includes deflutter compensation circuitry to prevent the record/reproduce process from degrading sensor dynamic range or introducing spurious flutter components in the sensor spectrum.

(U) Figure 2-3 is a block diagram of the demultiplexer system. The data channel from the recorder is conditioned in the tape playback amplifier and fed to the up-translator and 102 KHz phase-locked-loop.

(U) A standard phase-lock-loop consisting of a VCO, divider, phase detector and loop filter provides restored reference tones as needed from the filtered 102 KHz reference on the tape. A 1.2 KHz reference derived from this loop serves to frequency-lock the individual demultiplexer channel pairs. A 78 KHz reference obtained from the loop is used for data up-translation. The loop filter is made wide enough to track the recorder induced flutter on the 102 KHz reference. This flutter is detected by a discriminator and applied to the individual demultiplexer VCO's as an open-loop correction.

(U) The up-translator is identical to the down-translator in the multiplexer except that the input and output bandpass filters are reversed. The incoming data is mixed with a 78 KHz reference in a linear mixer and the sum frequency selected by the output filter.

UNCLASSIFIED

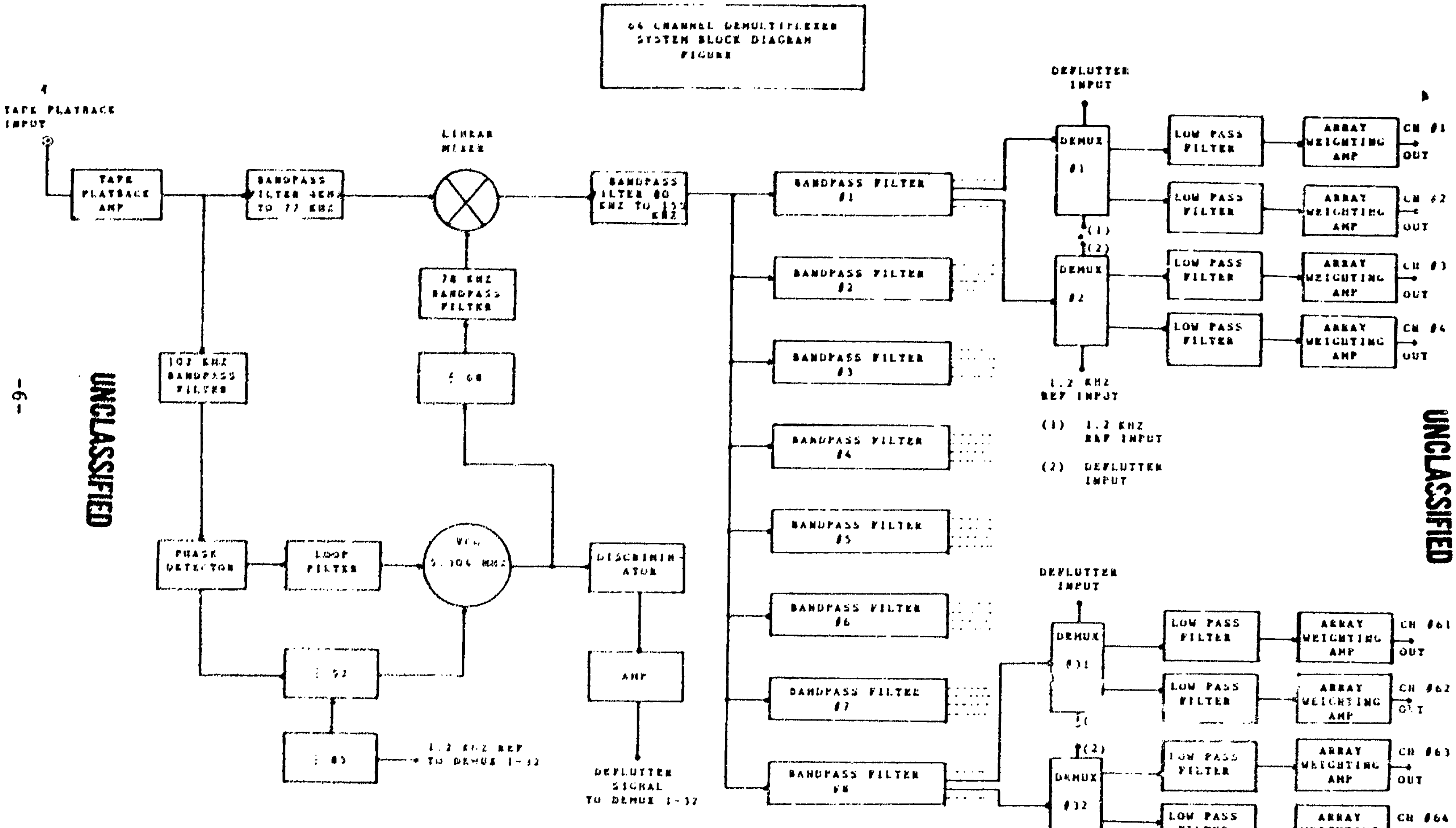

(U) FIGURE 2 1 SIXTY FOUR CHANNEL DEMULTIPLEXER SYSTEM BLOCK DIAGRAM (U)

UNCLASSIFIED

(U) The band is then divided into eight segments in a bank of bandpass filters. These filters lower the dynamic range requirements of each of the demultiplexers. Each filter passes four carriers to four respective demultiplexers.

(U) The 32 demultiplexers restore the individual sensor data. Each demultiplexer has a programmable phase-lock loop tuned to one of the 32 carriers. The incoming signal is passed through an AGC amplifier to in-phase and quadrature choppers (balanced mixers). The chopper difference frequency is selected in a 300 Hz low-pass filter. The AGC is controlled by the DC level out of the in-phase chopper. The DC level is a measure of the carrier amplitude and restores the system gain calibration regardless of the gain in the multiplexer, AGC amplifier or any gain differences in the tape recorder or various bandpass filter responses.

(U) 2.2.3 SPRAY BEAMFORMER DESCRIPTION (U)

(U) The data presented in this final report was processed through a Sanders Mini-computer Beamformer developed independently in 1974. Table 2-1 summarizes the pertinent characteristics. Although the SPRAY Beamformer was not developed with program funds, a description is included in this report to explain the data reduction procedures thoroughly.

(U) The SPRAY Beamformer has several interesting design features, including facile interaction with the operator, real time processing of long arrays at high resolution, parametric compensation of array deformation and on-line maintenance of test and recovery routines. The inclusion of these features made the SPRAY Beamformer a very useful tool both at sea during the MINYAKA and bearing stake sea tests and in the laboratory during data reduction of these sea tests.

(U) Figure 2-4, a block diagram of the SPRAY Beamformer, shows the simplicity afforded by the computer-based design. With the beamforming process realized in computer software, the hardware design is very straightforward. The 53 audio channels from the SPRAY Demultiplexer feed a 64-channel analog multiplexer coupled to a 12-bit analog-to-digital converter. The digitized samples are fed to a buffer inside the MIP-16 minicomputer via a direct memory access (DMA) interface. The MIP-16 processes samples from this DMA buffer, then passes the digitized beamformed data through a programmed I/O interface to a set of digital-to-analog converters buffered by a clock FIFO. The analog outputs of the D/A converters are lowpass filtered for sample interpolation before being sent to the input of the spectrum analyzer.

TABLE 2-1

(U) BEAMFORMER CHARACTERISTICS (U)

Number of Beams	4
Number of Input Channels	64
Beamforming Algorithm: Choice of One from the Software Library	Time Domain, Hydrophone Sample Storage, No Interpolation (Conventional Time-Domain Beamforming)
	Time Domain, Hydrophone Sample Storage, Output Sample Interpolation (Virtual Sampling Beamforming)
	Time Domain, Beam Sample Storage, No Interpolation (Partial Sums Beamforming)
	Time Domain, Beam Sample Storage, Output Sample Interpolation (Virtual Partial Sums Beamforming)
Sampling Rate	Physical Rates Programmable to 1200 Hz per Channel
	Synthetic Rates Programmable up to 13.2 KHz per Channel
Hydrophone Types	Omnidirectional or Limacon Element (Collocated Omnidirectional and Gradient Sensors for Array Image Lobe Suppression)
Operator Interface	Via Computer Terminal with Conversational Prompting and Short-Form Commands
Computer Type	Sanders Associates MIP-16 Minicomputer with 24K Words Core Memory and 1K Words Bipolar Semiconductor Memory

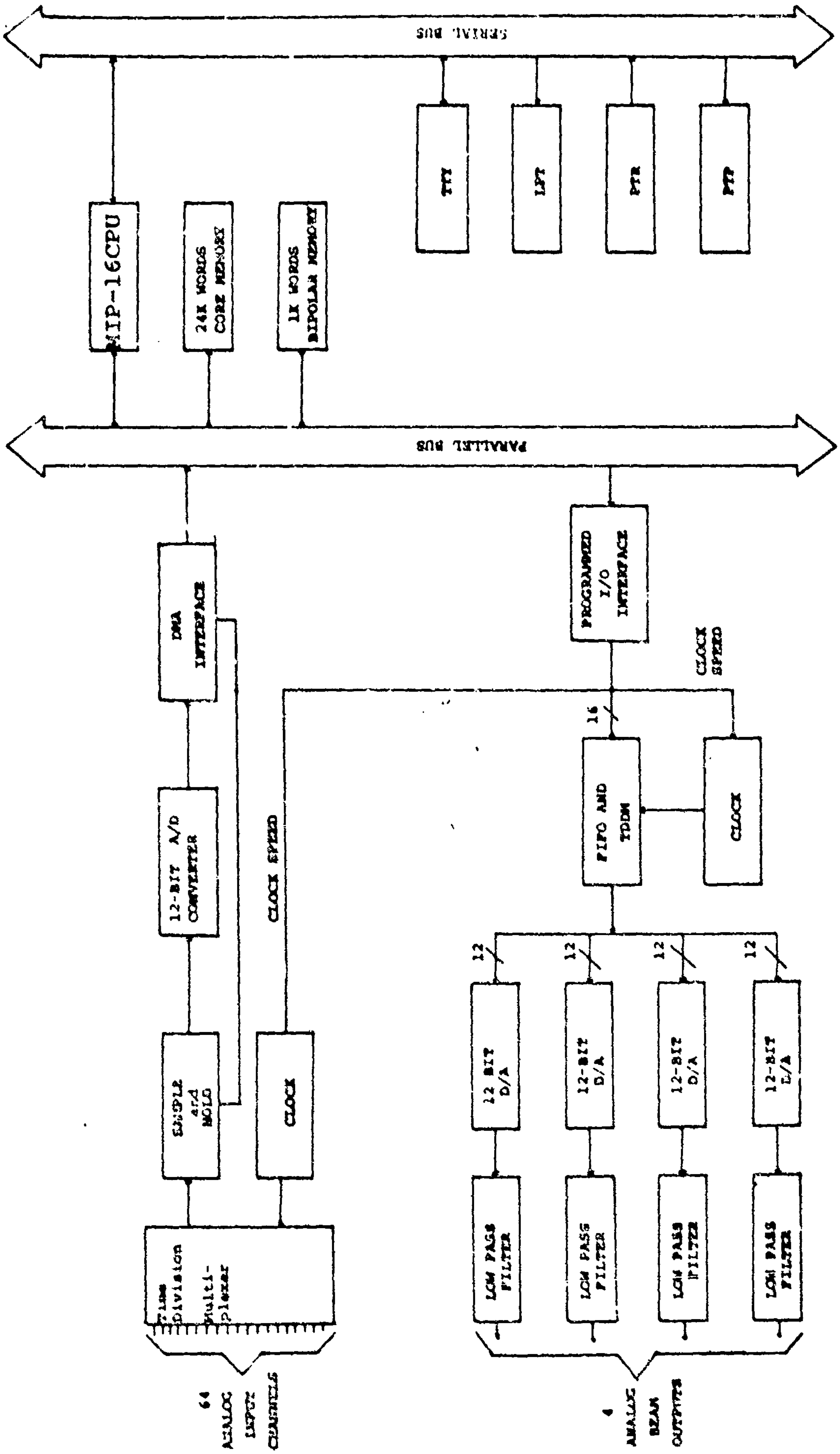

(U) FIGURE 2-4 SPRAY BEAMFORMER SYSTEM BLOCK DIAGRAM (U)

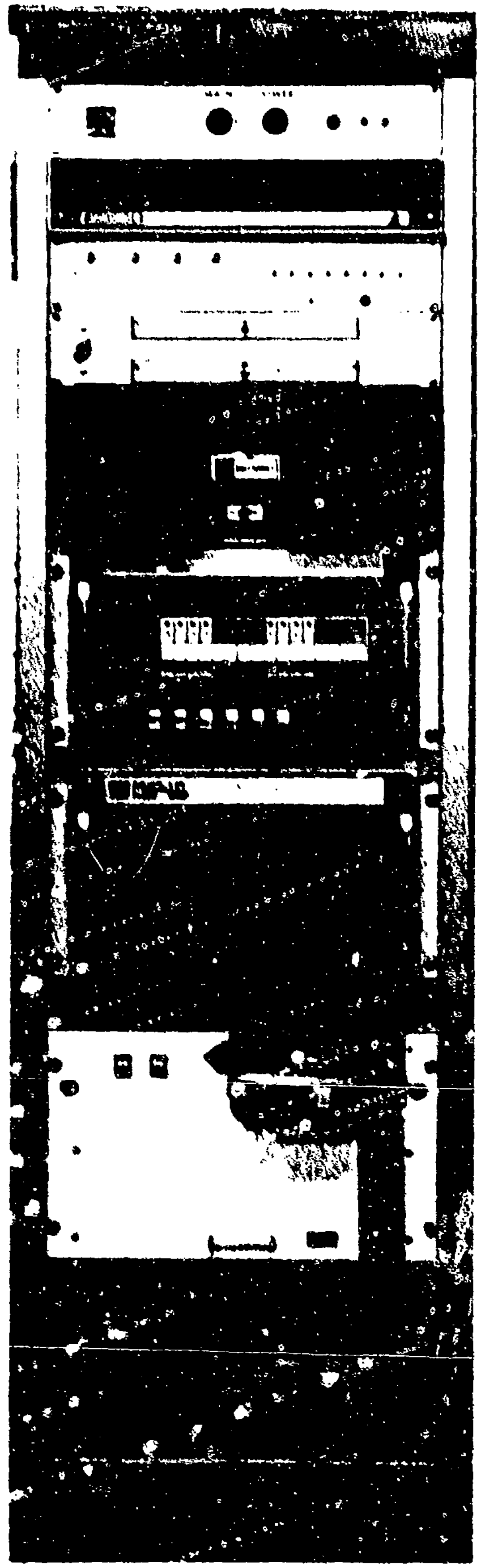

Figure 2-5

(U) Figure 2-5 is a photograph of the beamformer hardware. At the top of the rack in this figure, there is an interface from the SPRAY Demultiplexer to the MIP-16 minicomputer and from the MIP-16 to the beamformer's analog output ports. The MIP-16 is in the center of the rack, with a memory expansion enclosure beneath it.

(U) Use of a minicomputer greatly simplified the task of designing an effective operator interface. With the minicomputer in the system the monitoring and modification of the system parameters is done interactively. The beamformer operator converses with the computer to establish the steering angle, hydrophone locations, sound speed, etc. He then issues simple commands over a terminal to sweep the beams and locate the target-of-interest. With the computer automatically calculating and applying the proper channel delays and compensating for sound speed and curvature, the opportunity for operator error is minimized. The importance of this feature was brought out dramatically during the sea tests when live data was analyzed during high sea states.

(U) The beamformer software was designed to provide a real-time multiprogramming environment with a multiple priority interrupt structure. These software attributes permit the operator to generate tables and modify system parameters (e.g., steering angles, hydrophone assignments, etc.) without disturbing the real-time beamforming process. Thus, the operator can change the characteristics of one beam channel without causing any discontinuity in the other three beam channels. In addition to the foreground real-time and operator service tasks, several monitoring tasks execute in the background to detect and recover from momentary power failures and interface errors.

(U)2.2.4 DIGITAL SIGNAL PROCESSOR AND DISPLAY SYSTEMS (U)

(U) The Sanders-developed 6108 Digital Signal Processor was used as one of two spectrum analyzers and signal averages employed for this SPRAY, bearing stake, data reduction effort. This processor is a programmable analyzer system capable of processing up to three analog channels with a spectral resolution as low as 0.016 Hz. Absolute or relative level processing over a 96 dB dynamic range is provided by the system. Figure 2-6 is the 6108 Digital Signal Processor Block Diagram.

(U) The 6108 System accepts three channels of information within a 0 to 4800 Hz bandwidth and performs real-time processing of all channels. The input data is conditioned for conversion to 8-bit complex time samples (10-bit accuracy), 4096 complex words accumulated, converted to complex 32-bit frequency domain data,

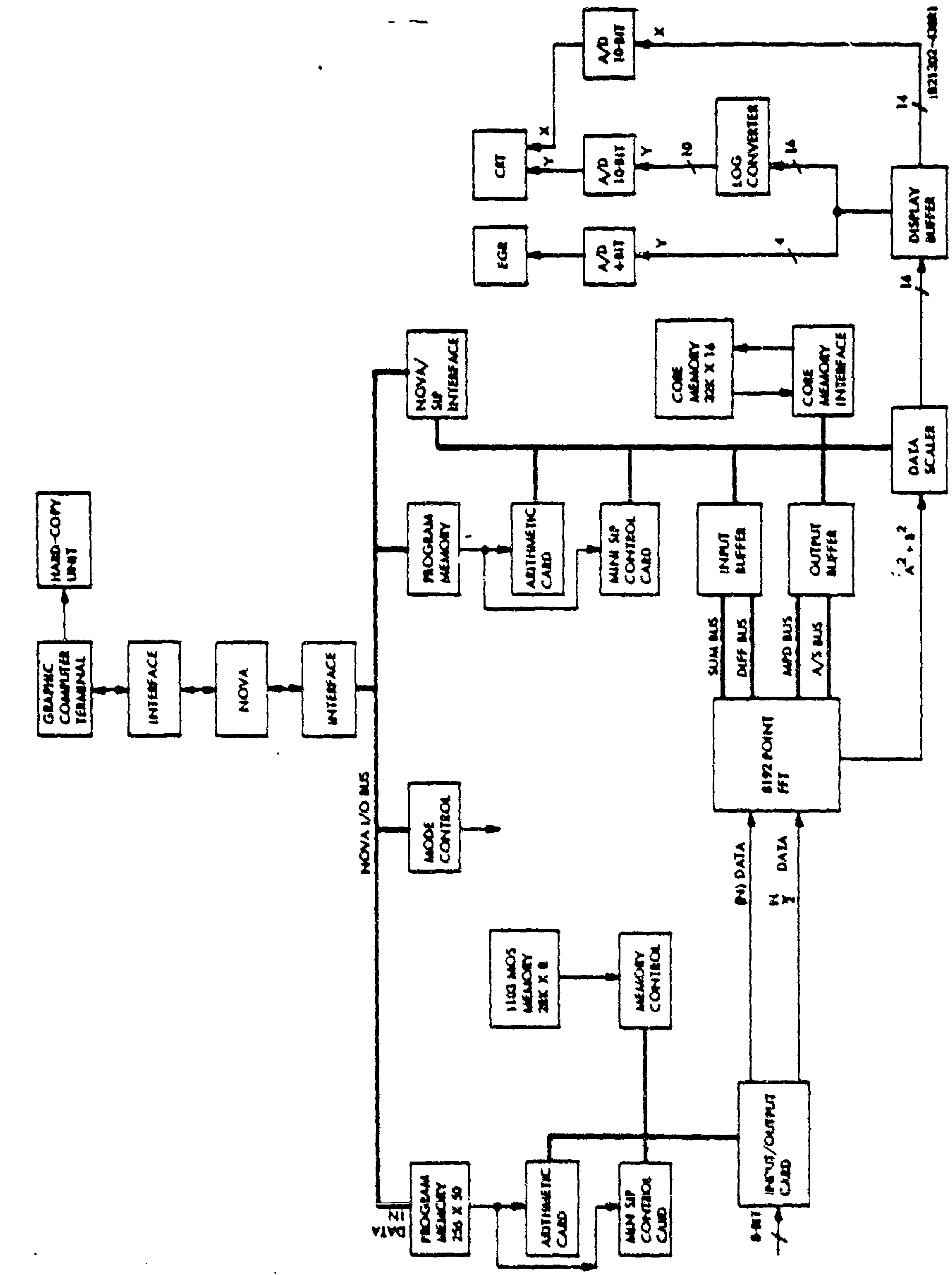

(U) Figure 2-6 Sanders-Developed 6108 Digital Signal Processor Block Diagram. (U)

detected by a linear function, integrated and sent to the NOVA computer as 16-bit words for subsequent formatting and output. In addition, the system's post processor uses a two-pass moving window algorithm to scale the 16-bit spectral data down to 4 bits for electrographic recording.

(U) The ALIU spectral data sent to the NOVA computer by the system's post processor are formatted and sent via a digital interface to a Tektronix 4002A Graphic Computer Terminal for display. Hard copies of each of the three processor channels ALIU outputs can be produced by means of a Tektronix 4601 Hard-Copy Unit.

(U) The Sanders developed MCPS-32A Digital Signal Processor was the second spectrum analyzer and signal averager used for this data reduction effort. This processor is an FFT Spectrum Analyzer with built-in frequency translation and post processing. Resolutions between 0.8 Hz and 0.0125 Hz may be used on up to 32 simultaneous analog inputs. The center frequency of the band to be analyzed may be selected in one Hz steps up to 3,000 Hz. Figure 2-7 is the MCPS-32A Block Diagram.

(U) Inputs are first filtered by a 2,400 Hz low-pass anti-aliasing filter. Each channel is then A/D converted to 12 bits and mixed with a digitally synthesized center frequency for translation. The resultant complex samples are digitally low passed filtered. Since complex data is used, a low pass is equivalent to a bandpass centered at DC and therefore determines the analysis bandwidth. 1024 complex words, 12 bit real, 12 bit imaginary and collected for each input. A 1024 point FFT then calculates the spectral content using a 4-point algorithm and 16 bit fixed point complex arithmetic. After envelope detection ALIU's are calculated using an RC or glossy filter algorithm whose time constant is operator controlled. The averaging is performed with 24 bit accuracy. Resultant data is converted to log format and displayed on a high resolution CRT display which provides accurate frequency reading and line level measurements. Since all calculations are in fixed point format and no AGC is employed, the output is calibrated with IVRMS at the input giving a 0 dB output reading. An analog output is available to develop uncalibrated (amplitude) hard copy X-Y plots of frequency vs amplitudes.

(U) 2.2.4.1 Processing Parameters (U)

(U) Table 2-2 lists the processing parameters used in producing the SPRAY ALIU and FRAZ data included in volumes 3 and 4, books A and B of this report. The word FRAZ is a shortened version of our coined word HISTOFRAZ, which means history of frequency and azimuth, for this particular illustration format.

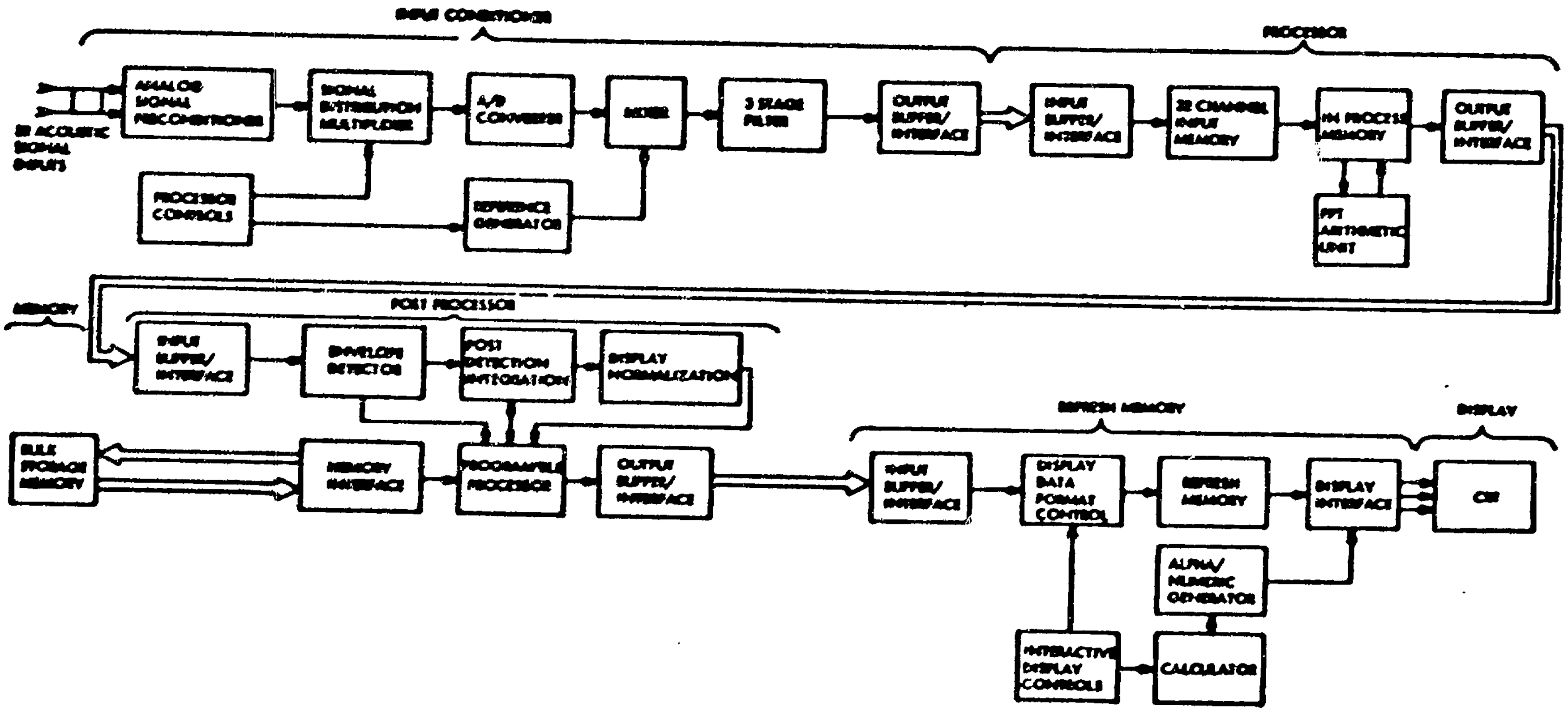

(U) Figure 7: Block Diagram (U)

UNCLASSIFIED

UNCLASSIFIED

TABLE 2-2

(U) PROCESSING PARAMETERS (U)

SANDERS 6108 PROCESSOR

Item	ALIU Data	FRAZ Data
Bandwidth	75 Hz*	300 Hz**
Resolution	1/32 Hz	1/8 Hz
Redundancy	x 2	x 8
Detector	Linear	Linear
Integration	320 Sec.	--
EGR Sweep Rate	--	1 Sec.

*When selecting a processing bandwidth, the operator must also select a center frequency for the system's digital translator. When processing ALIU data, two center frequencies were alternately used; one at 140 Hz (to obtain projector frequencies between 102.5 Hz and 177.5 Hz and one at 270 Hz (to obtain the projector frequencies between 232.5 Hz and 307.5 Hz).

**When processing the FRAZ data, a single center frequency of 150 Hz provided spectral outputs from 0 to 300 Hz (for 6108 processor only).

SANDERS MCPS-32 PROCESSOR

Item	ALIU Data	FRAZ Data
Bandwidth	76 Hz*	--
Resolution	0.1 Hz	--
Redundancy	None	--
Detection	Linear	--
Integration	320 Sec.	--

AN/AQA-5

Item	ALIU Data	FRAZ Data
Bandwidth	--	300 Hz***
Resolution	--	0.2 Hz
Redundancy	--	None
Detection	--	--
Integration	--	--
Sweep Rate	--	1 Sec.

***Only 10 Hz to 300 Hz available with this processor.

(U) 2.2.4.2 Processors Calibration (U)

(U) Prior to processing the SPRAY Sea Test Data, the 6108 Digital Signal Processor and Display System, and MCPS-32 Digital Signal Processor and display system were calibrated to verify acceptable operational accuracy. This calibration was conducted in two parts for the 6108 Processor and MCPS-32 Processor. The calibration of each system will be discussed separately.

(U) The first calibration test, of the 6108 Processor, was to check out the log conversion algorithm used in the NOVA Computer to convert the integrated spectral levels received from the 6108 post-processor memory to dB for display. This test was performed by manually loading a known digital step function into the NOVA Computer's core memory locations normally reserved for spectral data. The input step function was selected to produce an output having 6 dB steps. Once this data was loaded into core, the system software was initiated to produce the resulting output on the Tektronix Graphic Computer terminal. Figure 2-8 are results from the first step calibration. As this figure indicates, a high level of accuracy was achieved from this test, indicating an acceptable log conversion algorithm and proper data formatting by the system software.

(U) The second part of the system calibration used analog signals havin[illegible]n signal-to-noise ratios. These signals were produced by summing the ou[illegible]a white noise generator and a frequency synthesizer set to 100 Hz. The resulting analog signal was processed as if it were an output from the SPRAY Beamformer or Demultiplexer. The 6108 Digital Signal Processor was set up as outlined for ALIU data in paragraph 2.2.4.1. A series of individual calibration runs were made using simulated input SNR's ranging from +4 dB to +39 dB in 5 dB steps, (Appendix A, page A-2 thru A-13). Note that these SNR levels are referenced to the processor's resolution of 0.03 Hz. The raw ALIU outputs produced from these SNR calibration tests are included in Appendix A of this volume. Figure 2-9 summarizes the results of the SNR calibration runs. Note that for the eight SNR values tested, the worst-case error was only 0.6 dB. Similar worst-case errors exist when evaluating the calibration results of an absolute basis (refer to Appendix A, figures A-9 thru A-15).

(U) The Sanders MCPS-32 calibration was conducted somewhat differently than the Sanders 6108. The spectral displays of frequency versus amplitude are presented on

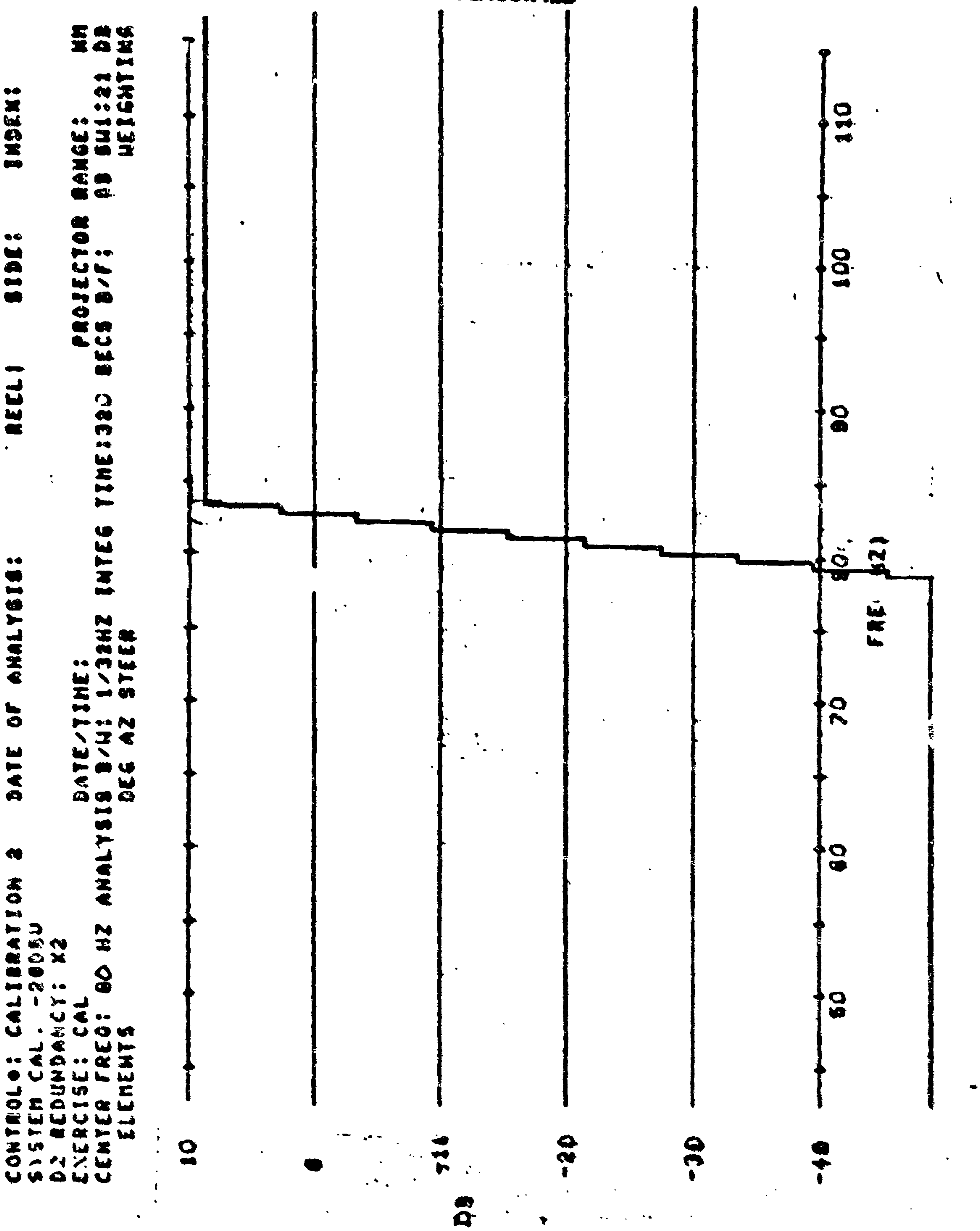

(U) Figure 2-9 Display Calibration Test Results. (U)

SYSTEM CALIBRATION

CALIBRATION RUN	INPUT SNR PER 1/32 Hz	INPUT TONAL LEVEL	OUTPUT SNR PER 1/32 Hz	ERROR
	dB	dBV	dB	dB
0	+4	-55	4.0	0.0
1	+9	-50	8.8	-0.2
2	+14	-45	13.7	-0.3
3	+19	-40	18.4	-0.6
4	+24	-35	23.6	-0.4
5	+29	-30	29.0	0.0
6	+34	-25	34.2	+0.2
7	+39	-20	39	0.0

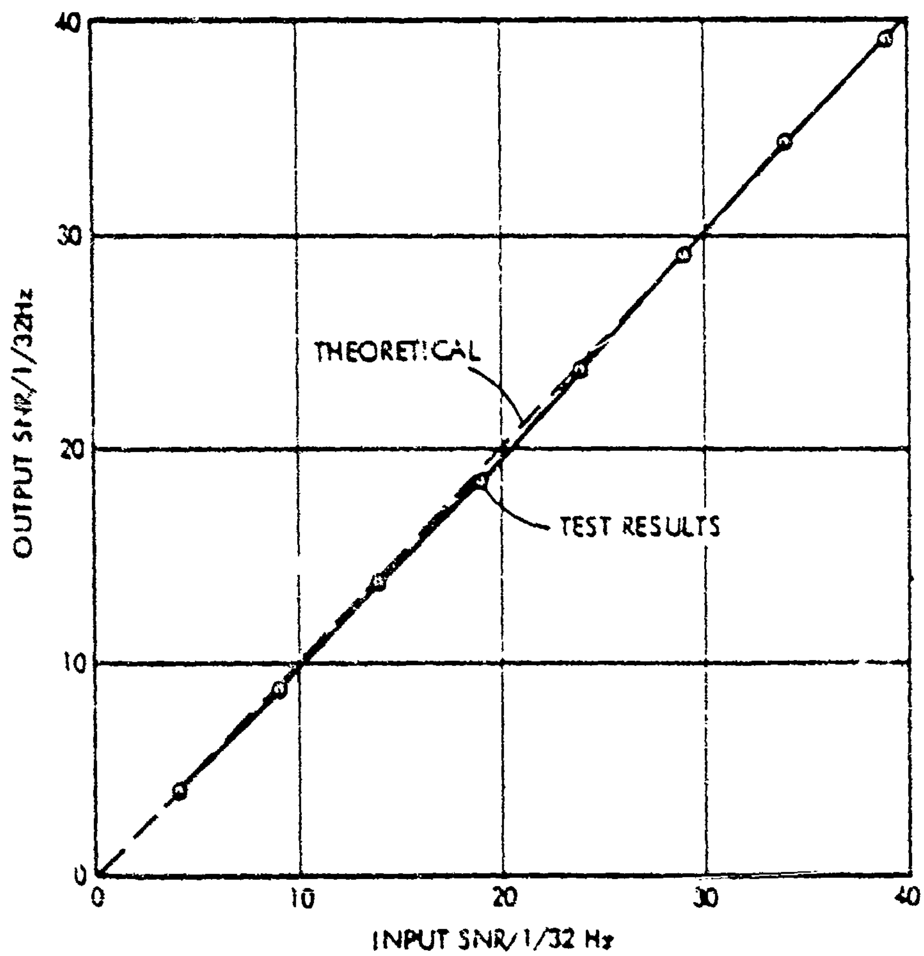

(U) Figure 2-9 Summary of SNR Calibration Run Results. (U)

a CRT. ALIU plots were developed and presented on the CRT. The plots consisted of a synthesized tonal of 300 Hz at a level of 1 VRMS. Each of the 32 channels was adjusted to read -10 dB for 1 volt. This was accomplished by slewing a cursor to the maximum level of the tonal selected and observing a digital readout on the CRT presentation. A screwdriver adjustment was set for each channel to read a -10 dBV. This procedure was performed at various intervals during the processing of the data points selected.

SECTION 3

(U) DATA PROCESSING PROCEDURES (U)

(U) This section details the procedures used in processing the raw data derived from the three sites of the SPRAY, Bearing Stake, Data Collection Sea Tests.

(U) 3.1 DATA POINT SAMPLE SELECTION APPROACH (U)

(U) During the three periods of the SPRAY Bearing Stake Sea Tests approximately 72 hours of SPRAY multiplexed data was recorded. Since it would be impractical to process all the tape recordings, the raw data was edited carefully to select twelve time segments from the three test periods (January, February and March, 1977). In-depth signal processing would be performed on the time segments selected. The following information was considered, in the order given, in determining the best time segments:

- .rojector to Receiver Positioning
  - Angular Position
  - Bearing Rate Change
  - Sequential Range Changes
  - Range
- Tape Recordings
  - Yes or No
  - Good or Bad
- Projector Data
  - On or Off
- Navigational Data
  - Accuracy
- Compass
  - Good or Bad

(U) Table 3-1 is the result of this time segment selection. In viewing in five categories considered for selection, table 3-1 represents the best time segments for in-depth analysis.

TABLE 3-1

(U) DATA POINT SAMPLE SELECTION SUMMARY (U)

Data Point	Test Date	Time Interval (ZULU) Start	Stop	Projector Range (NM)	Depth (FM)
1	1-19-77	1551	1556	91	1650
2	1-19-77	1600	1605	91	1650
3	2-7-77	0934	0939	175	1900
4	2-7-77	1019	1024	159	1900
5	2-7-77	1549	1604	110	1900
6	2-7-77	2033	2038	70	1900
7	2-8-77	0202	0207	28	1900
8	3-15-77	1501	1506	22	2800
9	3-15-77	2131	2136	72	2800
10	3-16-77	0633	0638	128	2800
11	3-16-77	0935	0940	122	2800
12	3-16-77	1148	1153	122	2800

(U) 3.2 SINGLE ELEMENT DATA (OMNI) (U)

(U) During the SPRAY MINYAKA data reduction effort, it was determined that variations existed between individual omnidirectional sensors. The variations from element to element exceeded 10 dB in some incidences. To obtain a more accurate or meaningful omni reference level, a procedure was adopted which provided a mean omni signal and noise level from all sensors along the array. This approach required processing all element individually and then calculating a mean signal level and noise level. During the SPRAY bearing stake data reduction, the same procedure was employed utilizing one half (every other) the sensors. It was determined that the mean omni level of all elements and the mean omni level of every other element (one half) was nearly identical.

(U) 3.2.1 MEAN OMNI SIGNAL LEVEL (U)

(U) Since the ALIU spectral outputs produced by the spray data reduction system were in units of dBV per 1/10 Hz or 1/32 Hz, a simple arithmetic average of the signal levels detected by each omni element would produce a mean omni reference level that was slightly biased. Therefore, the following equation was used to derive this omni reference:

$$\text{Mean Omni Signal Level} = 20 \log \left(\frac{\Sigma 10^{\left(\frac{A}{20}\right)}}{N} \right)$$

where

A = Amplitude of detected signal by each omni element, dBV

N = Number of omni elements used to calculate mean application of this equation merely converts the signal level detections from dBV to volts prior to taking the arithmetic average. The resulting average was then converted back to dBV, so that direct comparisons could be made between the beamformed ALIU signal levels and the resulting omni signal levels.

(U) 3.2.2 OMNI SNR DETERMINATION (U)

(U) The mean omni SNR reference was determined by using the mean omni signal level (described in paragraph 3.2.1) and the typical omni background noise level produced by the individual omni elements near the frequency-of-interest. Since both the signal level and noise level are expressed in units of dBV per 1/10 Hz or 1/32 Hz, a simple subtraction of the two values produced the omni SNR reference.

(U) 3.3 BEAMFORMED DATA (U)

(U) The SPRAY Beamformed performance data was processed over the same time intervals that the omni reference data was processed. This procedure permitted the direct comparison of the two sources of data to establish the degree of detection improvement realized by the SPRAY Beamforming process. Each spectral time period was started utilizing the time coded signal recorded on tape. By observing a time code readout, all spectrum analyzed plots, for any one time period selected, were commenced within one second of each other.

(U) The following subparagraphs detail the data reduction procedures used in producing the SPRAY Beamformed Operational Performance Data.

(U) 3.3.1 ELEMENT SELECTION (U)

(U) During the process of screening the quality of the data base recorded during the three test periods (paragraph 3.1), certain elements were noted to produce acoustic data that was marginal or of poor quality. These elements were omitted from the array aperture when processing the beamformed data. It should be noted that the omission of these faulty elements commonly required an aperture be selected for processing composed of a noncontiguous string of elements. Though this situation existed, every effort was made from beams utilizing contiguous elements.

(U) 3.3.2 FRAZ PROCESSING (U)

(U) The initial phase of processing the SPRAY Beamformed data consisted of producing frequency vs azimuthal (FRAZ) electrographic recordings (grams) of each time segment selected. Generation of these FRAZ recordings provided a qualitative evaluation of the arrays detection performance, azimuthal discrimination against interfering noise sources and the resulting maximum response axis (MRA) of the sound projectors from the array.

(U) When processing the FRAZ records, the beamformer's steering angle was incremented in steps that were a function of the total aperture size being processed. The following expression was used to establish these steering angle increments:

$$\theta_i = \sin^{-1}\left(\frac{i}{n}\right)$$

where

$i = -(N), -(N-1) \ldots 0 \ldots +N \ldots$ etc.

$N = (n_{high} - n_{low})/m$

and

n_{high} = Highest element number used

n_{low} = Lowest element number used

$m = 2$ (for overlapping beams at -4 dB points and uniform weighting)

The expression produces steering angle increments overlapping each other at their -4 dB points.

(U) The procedure used in generating the FRAZ records consisted of repeatedly reproducing a selected 5.4 minute segment of sea test data while incrementing the steering angle each 45 seconds. This procedure was adopted as a tradeoff between rewinding and reproducing the same section of tape for each steering angle (which took an excessive amount of time) and continually allowing the data tape to advance while incrementing the steering angle through its 180° of azimuth. Though this latter approach reduces the total processing time for each FRAZ, an excessive interval of time-history would have elapsed between the first and last steering angle increments; thus, this approach was unacceptable and the previously described tradeoff was used.

(U) 3.3.3 MAXIMUM RESPONSE AXIS (MRA) DETERMINATION (U)

(U) Having produced the FRAZ recordings (discussed in paragraph 3.3.2), an approximate MRA steering angle could be derived for each time segment sample selected for processing. These approximate MRA's were used as "starting points" in the process of establishing accurate MRA steering angles for each data sample.

(U) A typical MRA determination was achieved by performing a series of ALIU processing runs on the beamformer otuput. Steering angles near the MRA picked off the corresponding FRAZ grams were used in making these processing runs. The signal level of each projector frequency displayed on the resulting ALIU spectral displays was then plotted as a function of steering angles used to create the data. This technique produced the actual beam pattern realized by the SPRAY array at each detected projected frequency. The steering angle that produced the maximum projector frequency signal level was then noted as the MRA for that respective data segment.

(U)3.3.4 BEAMWIDTH DETERMINATION (U)

(U) The measured beam patterns produced during MRA determination (discussed in paragraph 3.3.3) were also used to determine the respective beamwidths produced by the spray array. These beamwidths were established by noting the -3 dB points on either side of MRA for each projector frequency, and by differencing the steering angles associated with these -3 dB points.

(U)3.3.5 SIGNAL LEVEL CORRECTION (U)

(U) Two corrections were applied to various signal levels. The MRA signal levels derived by processing the beamformer outputs are somewhat depressed due to the $4F_h$ sampling rate used by the beamformer. This sample rate causes gross phase quantization errors; particularly at the higher projector frequencies. The degree of MRA signal level depression can easily be computed by accounting for the exact phase errors imposed during beamforming. Such calculations were made for each MRA steering angle and projector frequency, and have been applied to the beamformed signal levels and SNR levels tabulated in Section 1 of volumes 3 and 4, book A and B, respectively.

(U) The signal-to-noise ratio algorithm calculates the estimated input S/N relative to a selected analysis bandwidth (ABW) from the measured output post detection S/N. The algorithm was employed to reflect the fact that MCPS-30 signal processor uses a linear detector.

(U) Fundamentally, the algorithm measures the difference between the detected signal level and the noise mean at the detector output, and using the detector transformation converts this difference into an input S/N. This is discussed in the following paragraphs.

(U) Linear Detector S/N Algorithm (U)

(U) The mean value of the envelope of a linear detector is:

$$\overline{E}_{S+N} = \sqrt{\frac{\pi}{2}}\,\sigma_e^{-y/2}\left[(1+\frac{\gamma}{2}\,I_o\,\frac{\gamma}{2}) + \gamma I_1\,(\frac{\gamma}{2})\right] \quad (1)$$

where

γ is the input SNR measured in the analysis filter bandwidth

σ is the RMS noise level in the analysis filter bandwidth

$$[\text{Note that when } \gamma = 0\ \overline{E}_N = \sqrt{\frac{\pi}{2}}\,\sigma\ .] \quad (2)$$

$I_0(X)$ and $I_1(X)$ are the bessel functions of orders zero and one respectively.

(U) Conceptually one could use equation (2) to obtain an estimate of σ from E_N which is known because of the thresholding. Then equation (1) could be used to determine γ by solving for σ. However, because of the non-linear behavior of $I_0(X)$ and $I_1(X)$, this approach is not practical.

(U) Therefore, a computer study was made using equations (1) and (2) in which the ratio E_{S+N}/E_N was plotted in dB vs γ. (See figure 3-1.)

(U) The relationship was then used to define sixteen (16) regions in which linear approximation to the graph were subsequently used.

(U) The algorithm itself, therefore proceeds as follows. The values stored in the record for E_{S+N} and E_N are converted to dB and then the quantity $E_1 = E_{S+N} - E_N$ is calculated.

(U) The value of E_1 is then used with the proper linear approximation to calculate γ. The value of γ is then converted relative to a desired analysis bandwidth.

(U) The regions used for linear approximations are listed in figure 3-1.

(U) 3.3.6 BEAMFORMED SNR DETERMINATION (U)

(U) The beamformed SNR values quoted in volume I of this report are for MRA steering angles only. As explained previously, these SNR values have been corrected to

Figure 3-1:

(U) LINEAR DETECTION CORRECTION FACTOR (U)

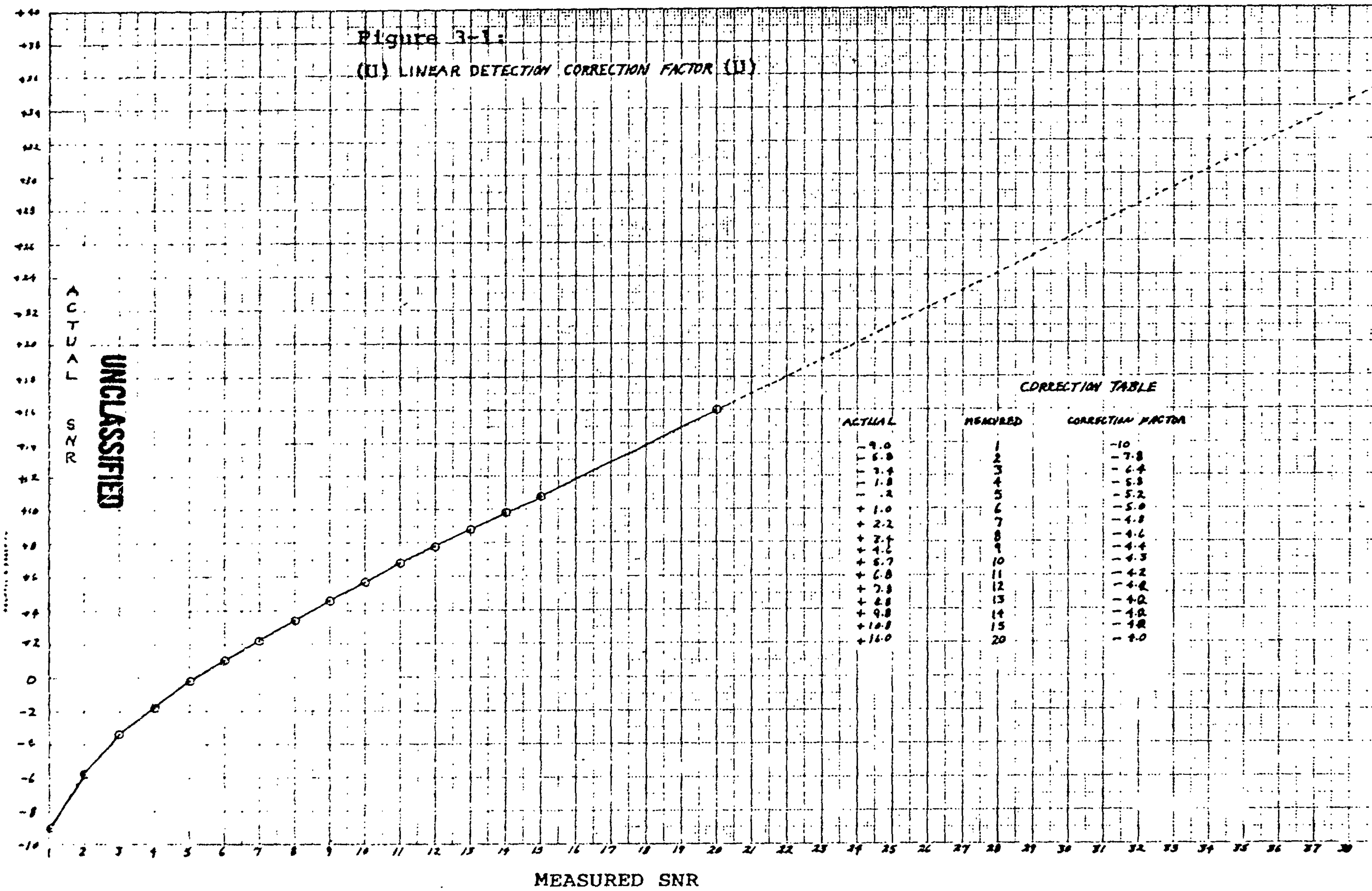

ACTUAL	MEASURED	CORRECTION FACTOR
−9.0	1	−10
−5.8	2	−7.8
−3.4	3	−6.4
−1.8	4	−5.8
−.2	5	−5.2
+1.0	6	−5.0
+2.2	7	−4.8
+3.4	8	−4.6
+4.6	9	−4.4
+5.7	10	−4.3
+6.8	11	−4.2
+7.8	12	−4.2
+8.8	13	−4.2
+9.8	14	−4.2
+10.8	15	−4.2
+16.0	20	−4.0

compensate for known phase quantization errors, linear detection processing gains, beamformer attenuations, and a variation in the MCPS-32 calibration. The technique used in arriving at a background SNR is nothing more than noting the narrowband signal level at MRA, applying the various amplitude corrections, estimating the background noise level at the frequency of interest and differencing the corrected signal level and noise level.

(S) 3.4 COMPASS DATA (U)

(U) Signal processing of the SPRAY compass data was performed to obtain the longitudinal heading of the array. The resulting array headings were combined with the MRA steering angles produced at each of the data points, and finally compared with the test navigation data to determine the degree of bearing accuracy achieved by the SPRAY array. Table 3-2 lists the data developed to compute the bearing accuracy realized with the SPRAY array.

TABLE 3-2

(S) BEARING DATA FOR SPRAY ACCURACY CALCULATIONS

Data Point	Date	Time	Compass Bearing	Navigation Bearing	Spray Bearing	Steering Angle
1	1-19-77	15512	037°	250°	248.5°	-58.5°
2	1-19-77	16002	048°	250°	259°	-59°
3	2-7-77	09342	260°	322°	325°	+25.5°
4	2-7-77	10192	275°	323°	333°	+32°
5	2-7-77	15492	278°	322°	319°	+49°
6	2-7-77	20332	000°	318°	285°	+15°
7	2-8-77	02022	117°	293°	218°	-21.5°
8	3-15-77	15012	*	305°	**	+20°
9	3-15-77	21312	*	314°	**	+51.5°
10	3-16-77	06332	*	323°	**	+61.5°
11	3-16-77	09352	*	335°	**	+62°
12	3-16-77	11482	*	342°	**	+62°

*No compass data this data point

**Unable to calculate SPRAY bearing

(U) The following paragraphs describe the data reduction procedures used in processing the array compass data, as well as the results produced at each data point selected for analysis.

(U) 3.4.1 PROCESSING INSTRUMENTATION (U)

(U) The SPRAY compass produced two channels of data which were multiplexed onto the composite signal and ultimately recorded on the analog tape recorder. One of the two signals was the compass phase reference, and the other signal was the actual compass phase signal. The two channels of compass data were recovered from the tape recorded multiplexed SPRAY signal via the SPRAY Demultiplexer. Both the compass reference and the compass phase signals were sine waves displaced in phase by an amount porportional to the compass heading.

(U) Figure 3-2 is the compass data processing instrumentation block diagram.

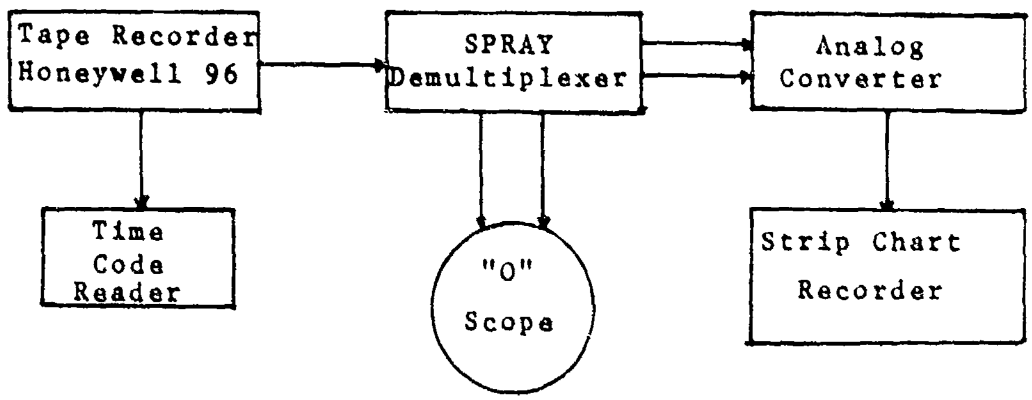

Figure 3-2

(U) The measured phase angle between the compass reference signal and phase signal was subsequently applied to the appropriate compass calibration curve to obtain the magnetic heading of the compass and/or array at each data point selected for processing.

(U) The resulting magnetic headings of the array were then combined with the MRA steering angles, for each data point, to convert the relative array steering angle to magnetic bearings to the projector ship. These magnetic bearings were finally

compared with the test navigation data to determine the overall pointing accuracy of the SPRAY array. (Volume 1, figures 2-9 thru 2-15.)

(S) 3.4.2 EVALUATION OF SPRAY BEARING ACCURACY (U)

(S) Figures 2-8/9 in volume I are plots of array bearing vs navigation bearing for the January, 1977 SPRAY Sea Test in the Gulf of Oman (Test Site 1A). The water depth was 1650 fathoms. Figures 2-10/14 in volume I are plots of the array bearing vs navigation bearing for the February, 1977 Spray Sea Test in the Arabian Sea (Test Site 3). The water depth was 1900 fathoms at this test position. At Test Site 4 (Somali Abyssal Plain) in March, 1977; no usable compass data was obtained from the tape recordings. Documentation during the testing noted that the compass data was excessively noisy, consequently no bearing accuracy evaluations can be made from this deep water site (2800 FMS).

(U) The bearing data plotted in figure 2-7A and figure 2-7B, of volume IB, was obtained from figures 3-3 thru 3-8. The array headings, broadside bearings, projector navigation bearings, and projector array bearings, were plotted in that sequence and spray bearing accuracy was determined. The projector navigation bearing and projector bearing were then replotted in figures 2-7A and 2-7B, volume I.

(S) The spray tracking accuracy was very good for Test Site 1A. The tracking accuracy obtained at Test Site 3 was good for data points 3, 4, and 5. The tracking errors for data points 6 and 7 were quite large, 33° and 65° respectively. The array heading was continuously monitored on a compass during time periods that the array was in the water. Late in the afternoon of 7 February, 1977 the array was observed to be processing in a clockwise direction. By early morning of 8 February the array had completed 360° of rotation. In viewing the compass, strip chart, presentation (figure 3-7), it would appear that this rotation commenced about 2027Z. The strip chart recording of tape 15 of 7 February, 1977 indicates the change in compass heading started at 2027Z and changes approximately 26° during the next 40 minutes. The large discrepancies in array tracking could possibly have resulted from array curvature during this compass swing period.

(U) As was the case during the MINYAKA Spray Sea Tests, the compass was mounted on the deployment tug and not directly on the array. Angular motion of the tug relative to the array may have contributed to any bearing inaccuracies. In the final system configuration the compass will be mounted directly in the array and any possible error resulting from an angular displacement will be eliminated.

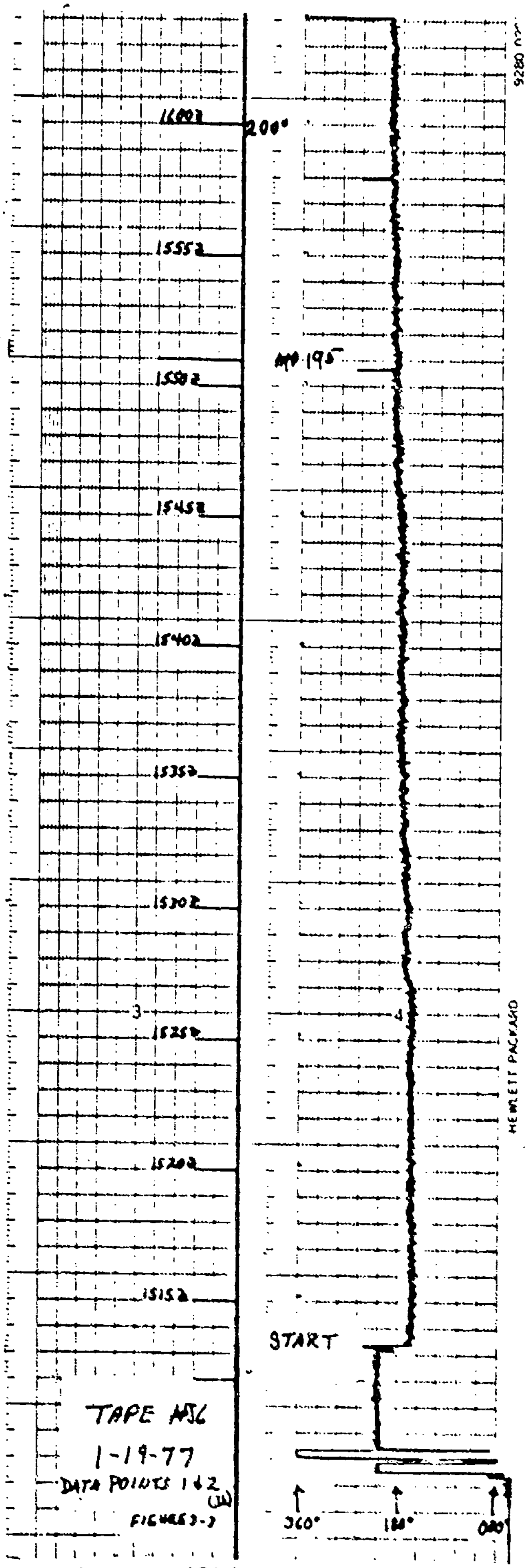
1600Z
200°
1555Z
195°
1550Z
1545Z
1540Z
1535Z
1530Z
1525Z
1520Z
1515Z
START
TAPE #36
1-19-77
DATA POINTS 1 & 2
360°
180°
000
HEWLETT PACKARD
9280

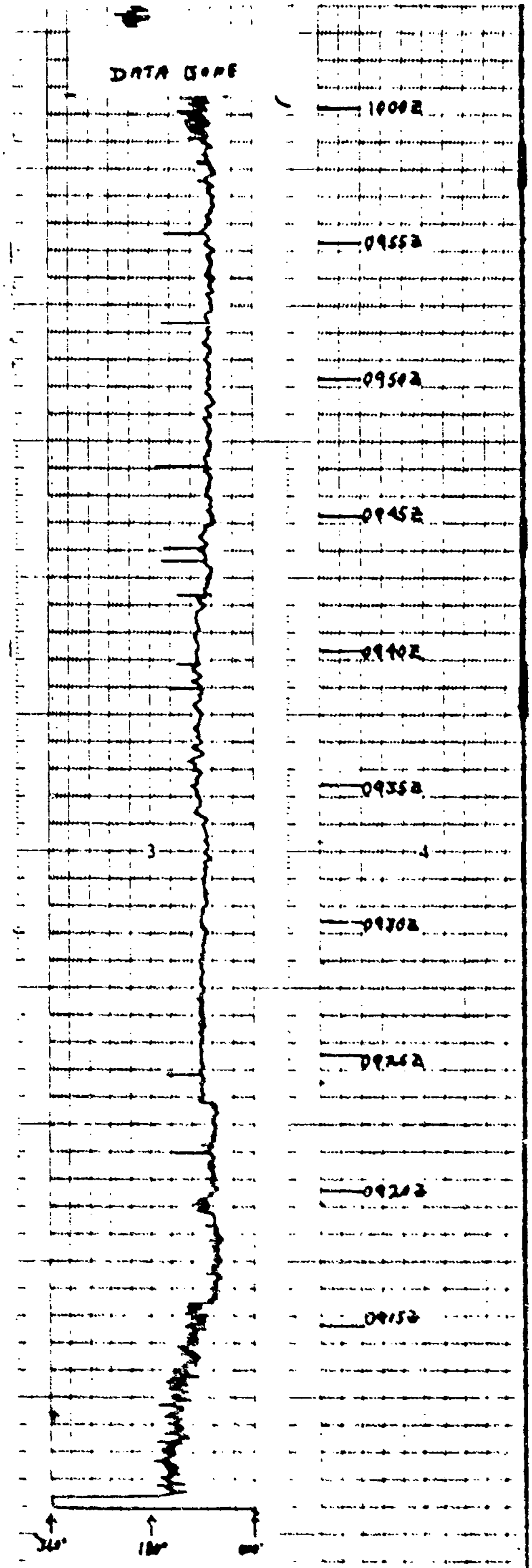

(U) TAPE HF14
2-7-77
DATA POINT 3 (U)

FIGURE 3-4

UNCLASSIFIED

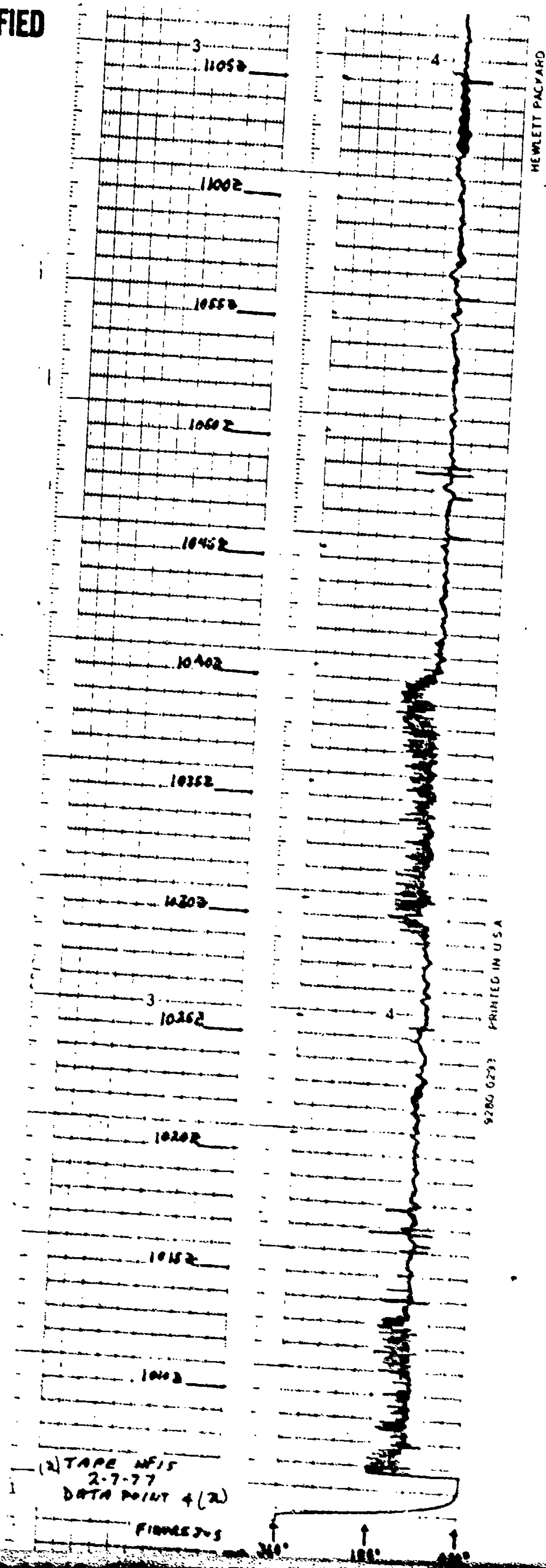

UNCLASSIFIED

UNCLASSIFIED

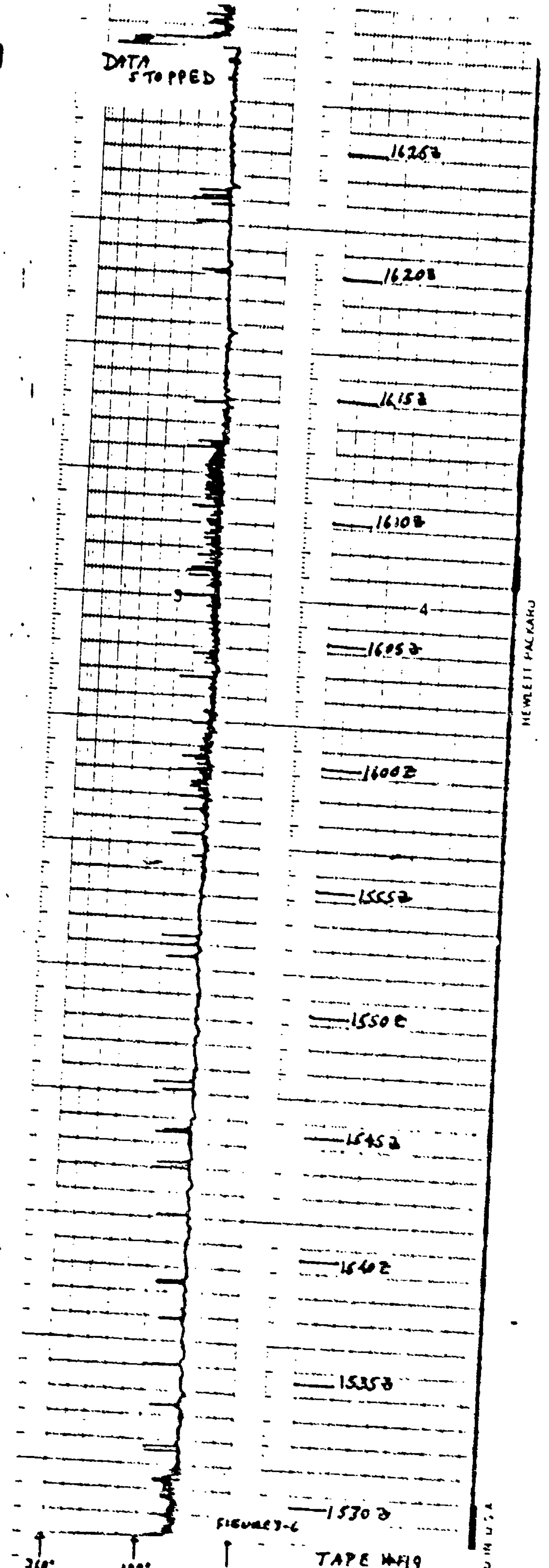

FIGURE 3-6

TAPE HF19
2-7-77
DATA POINTS (U)

UNCLASSIFIED

UNCLASSIFIED

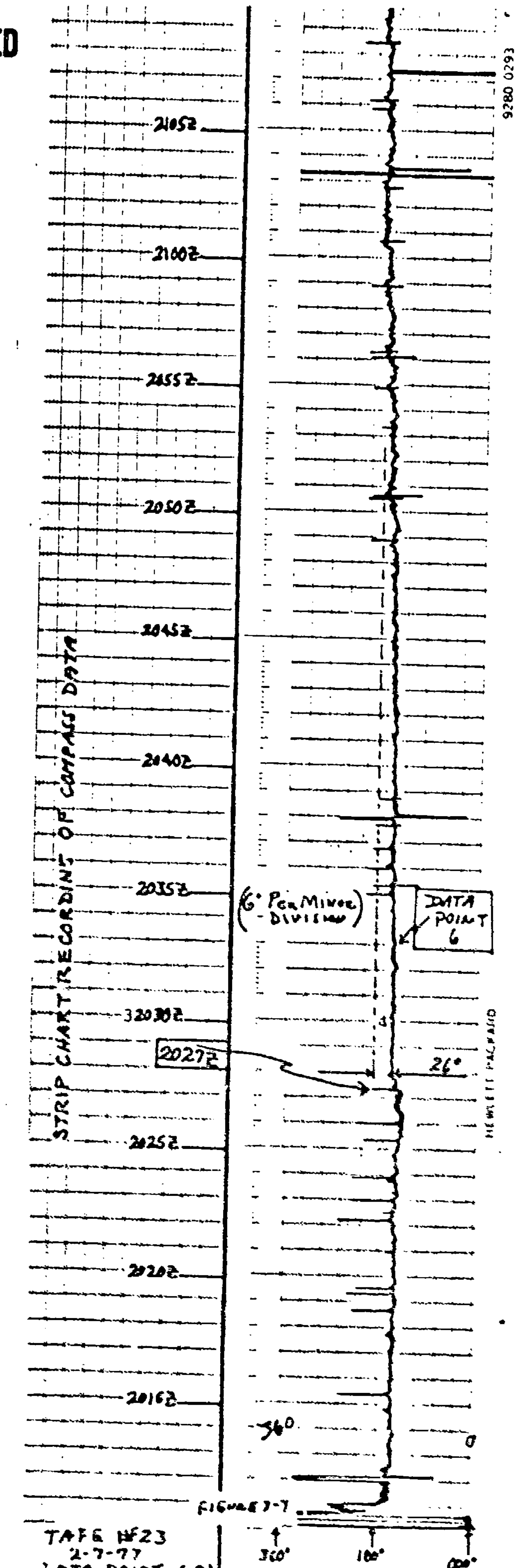

FIGURE 7-7

UNCLASSIFIED

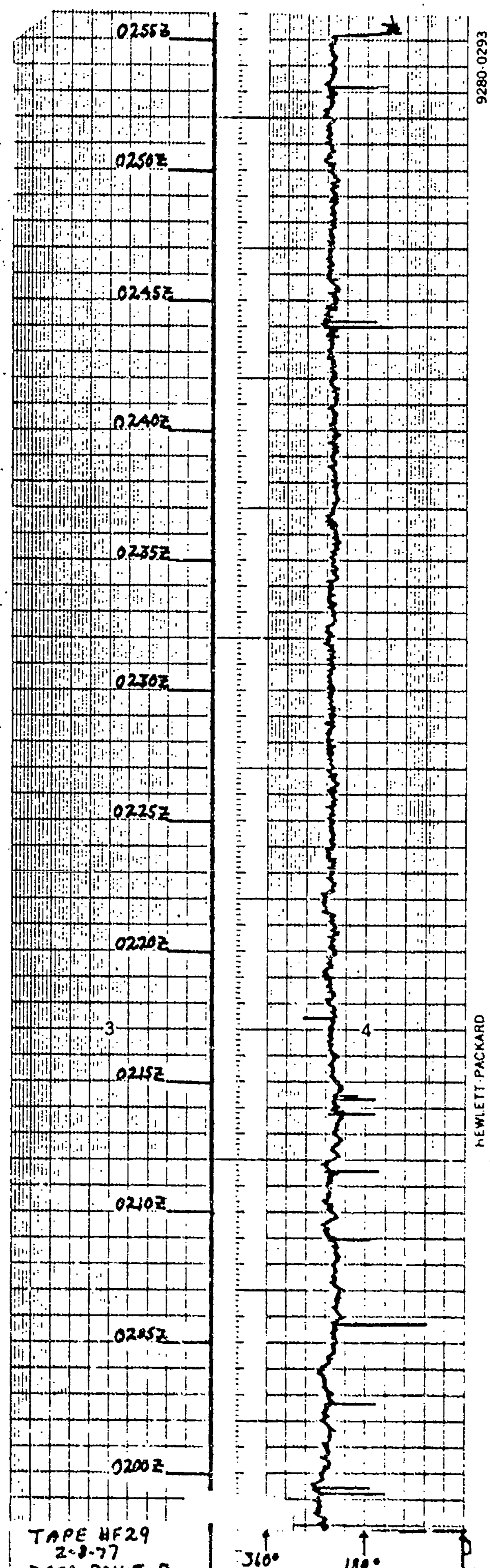
0255Z
0250Z
0245Z
0240Z
0235Z
0230Z
0225Z
0220Z
0215Z
0210Z
0205Z
0200Z
3
4
9280-0293
HEWLETT-PACKARD
TAPE HF29
2-8-77
DATA POINT 7
360°
180°
000°

FIGURE 3-8

SECTION 4
(U) MEASURED/THEORETICAL PERFORMANCE EVALUATION (U)

(U) 4.1 SIGNAL GAIN (U)

(U) Signal gain performance data was produced from the raw maximum response axis (MRA) beamformed processing results described in Section 3 of this volume. These signal gain results were derived for three aperture sizes for each of the 12 data points selected for processing. The aperture sizes selected were 16 elements, 32 elements, and maximum aperture (varied between 48 elements and 52 elements).

(U) The measured gain performance data was ultimately compared with the theoretical gains expected from a linear array such as SPRAY.

(U) 4.1.1 SIGNAL GAIN VERSUS NUMBER OF BEAMFORMED ELEMENTS (U)

(U) The signal gain performance of the SPRAY array was obtained by using the measured MRA signal level data at each projector frequency, and applying the amplitude corrections to compensate for the gains and attenuations resulting from the beamforming process and signal processing. The corrected signal level data was then referenced to the corrected mean omni signal level, merely by differencing the two sources of data at corresponding times and frequencies. The resulting data was then plotted as a function of the respective aperture sizes. A separate signal gain plot was prepared for each detected projection frequency used during the tests. Refer to figures A-1 thru A-24 volume I for results obtained at the three test sites.

(U) The theoretical signal gain curve included on these plots was derived by striking a 6 dB per octave line originating at the 1 element aperture point.

(U) 4.2 ARRAY GAIN (U)

(U) Array gain performance data was produced from the raw MRA beamformed processing results described in Section 3 of this volume. These array gain results were derived for three aperture sizes and each frequency at the data points selected for processing. The aperture sizes selected were 16 elements, 32 elements, and maximum aperture (varied between 48 and 52 elements).

(U) The measured array gain performance data was ultimately compared with the theoretical gains expected from a linear line array such as SPRAY. The following paragraphs describe the procedures used to produce the 2 types of array gain performance comparisons.

(U) 4.2.1 ARRAY GAIN VERSUS NUMBER OF BEAMFORMED ELEMENTS (U)

(U) The array gain performance of the SPRAY array was obtained by using the measured MRA signal-to-noise ratio (SNR) data at each projector frequency. Note that the SNR data had been corrected for any gains or attenuations realized during spectrum analyzing or beamforming processes. The corrected beamformed SNR data was then referenced to the corrected mean omni SNR data, merely by differencing the two sources of data at corresponding times and frequencies. The resulting data was then plotted as a function of the respective aperture sizes. A separate array gain plot was prepared for each detected projected frequency used during the tests. Refer to figures A-1 to A-4 in volume I for the 1650 fathom results, figures A-5 to A-14 for the 1900 fathom results, and figures A-15 to A-24 for the 2800 fathom results.

(U) The theoretical array gain curve included on these plots was derived by striking a 3 dB per octave line originating at the 1 element aperture point.

(U) 4.3 <u>BEAMWIDTH</u> (U)

(U) The beamwidths realized by processing the SPRAY data at the various projection frequencies were compared to theoretical beamwidths. This process was performed for three aperture sizes at each data point selected for processing. The aperture sizes selected were 16 elements, 32 element and maximum aperture (varied between 48 elements and 52 elements).

(U) 4.3.1 MEASURED BEAMWIDTH VERSUS THEORETICAL BEAMWIDTH (U)

(U) The measured beamwidths produced by the SPRAY array were compared to the theoretical beamwidths as a function of frequency and aperture size. These comparisons were made by plotting the measured beamwidths and theoretical beamwidths at corresponding frequencies against like aperture sizes. A separate comparison plot was made for each frequency and aperture size and included the 12 data points selected for processing. Both the measured and theoretical beamwidths were normalized to broadside equivalent prior to plotting. Refer to the plots in figures 2-17 to 2-25 in volume I for the results. The theoretical beamwidths included on these plots were analytically derived using well known linear array theory for various steering angles.

UNCLASSIFIED

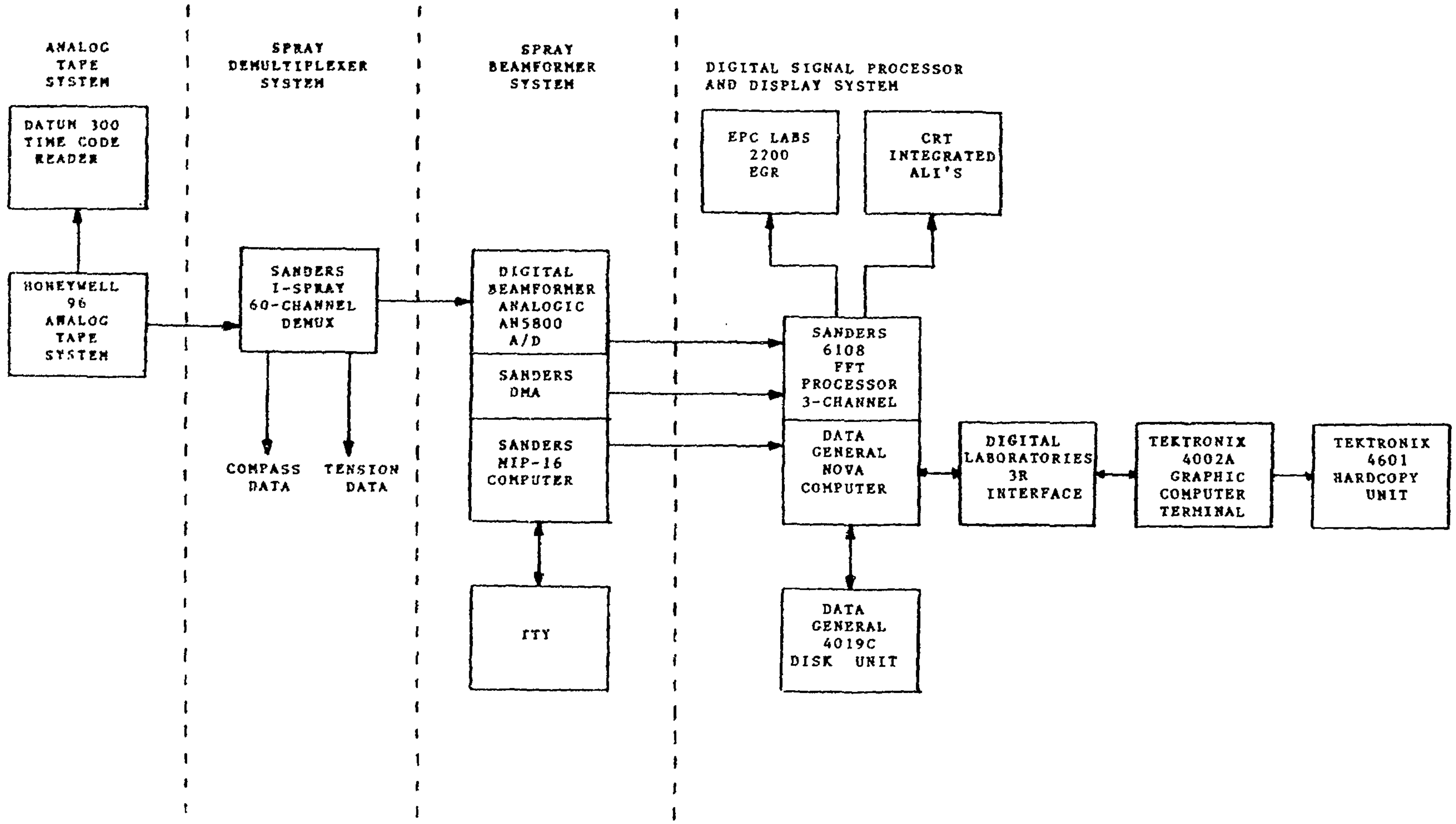

FIGURE 2-1 DATA PROCESSING INSTRUMENTATION BLOCK DIAGRAM

UNCLASSIFIED

UNCLASSIFIED

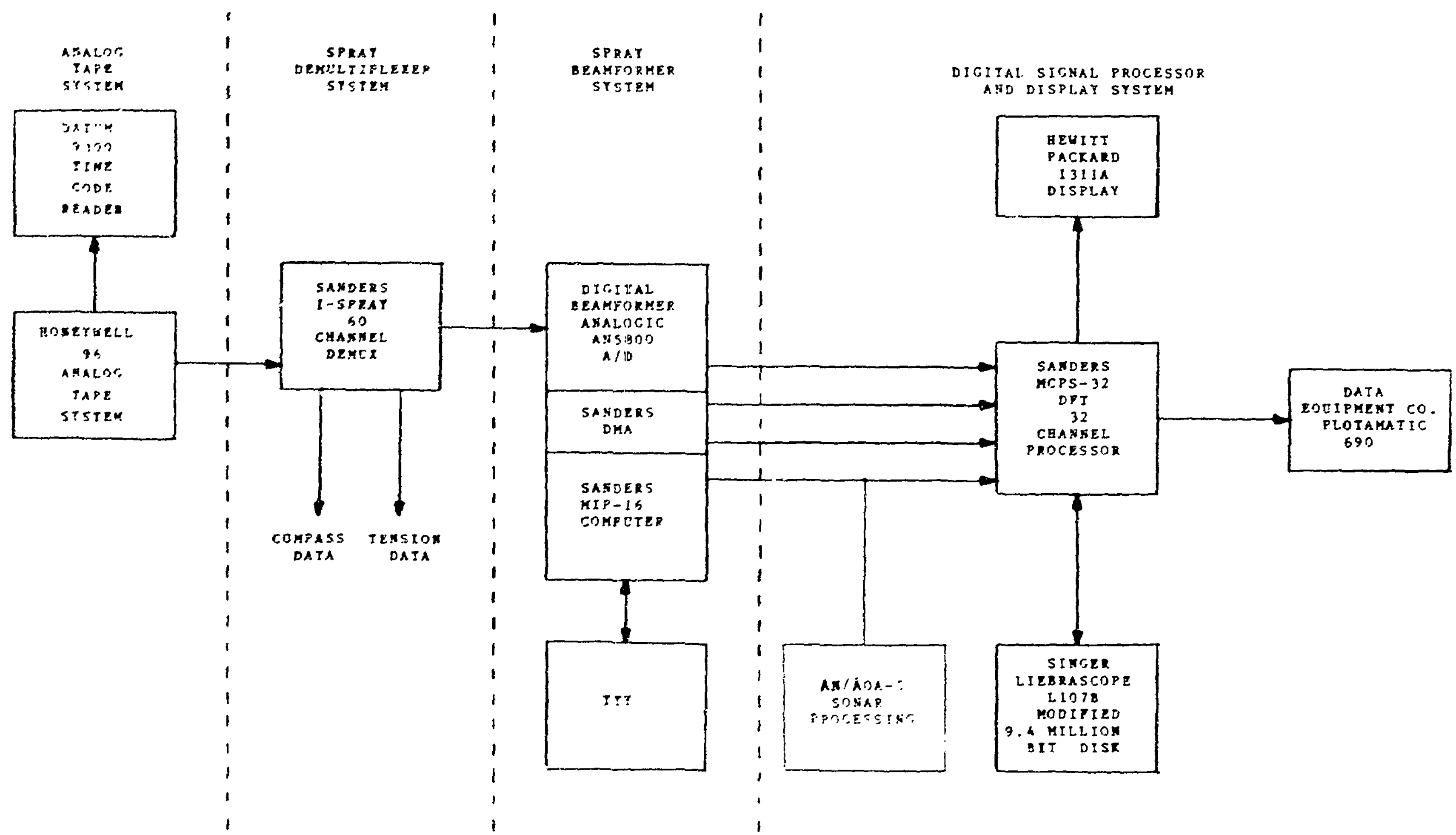

FIGURE 2-2 DATA PROCESSING INSTRUMENTATION BLOCK DIAGRAM

UNCLASSIFIED

UNCLASSIFIED

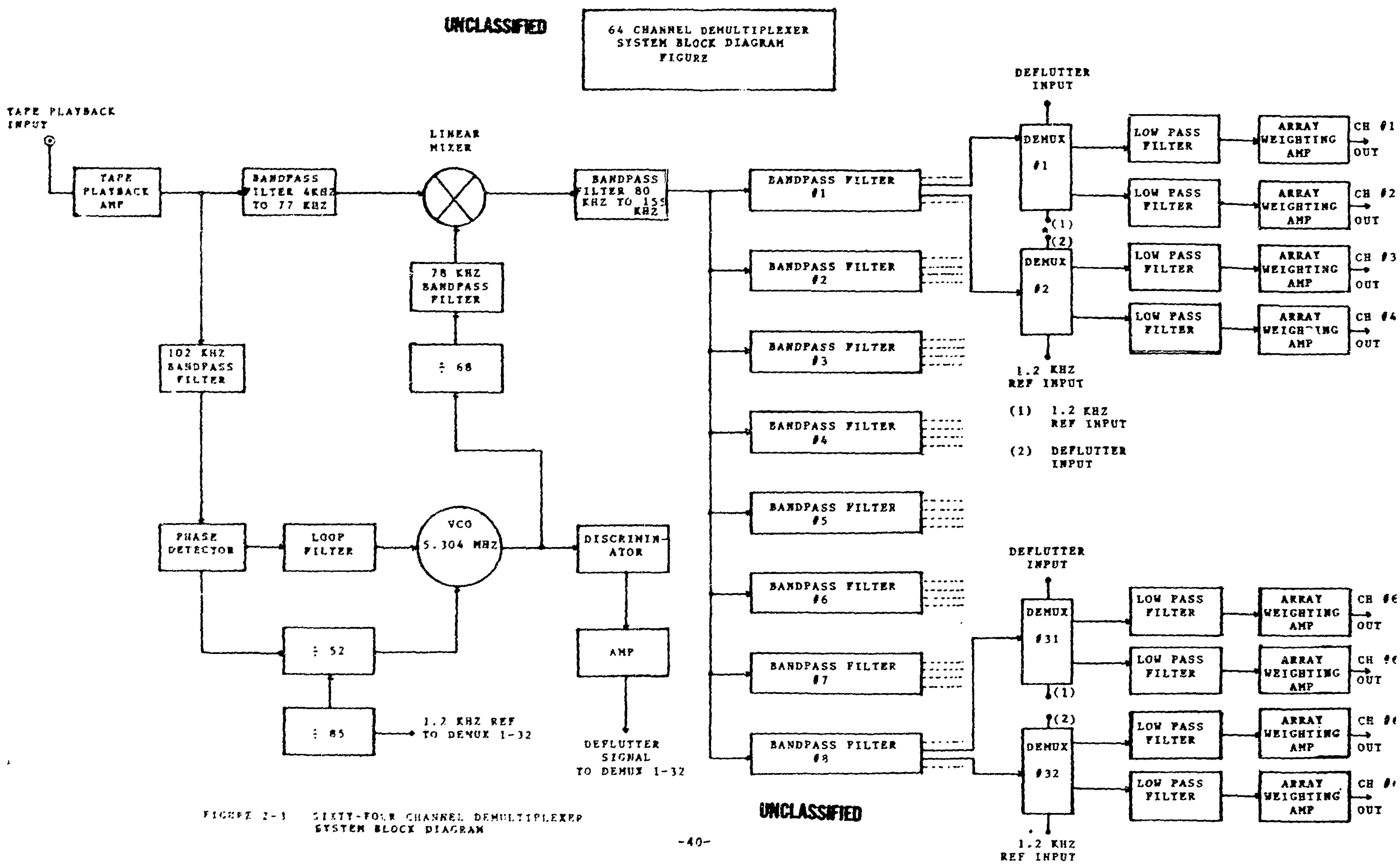

FIGURE 2-1 SIXTY-FOUR CHANNEL DEMULTIPLEXER SYSTEM BLOCK DIAGRAM

UNCLASSIFIED

UNCLASSIFIED

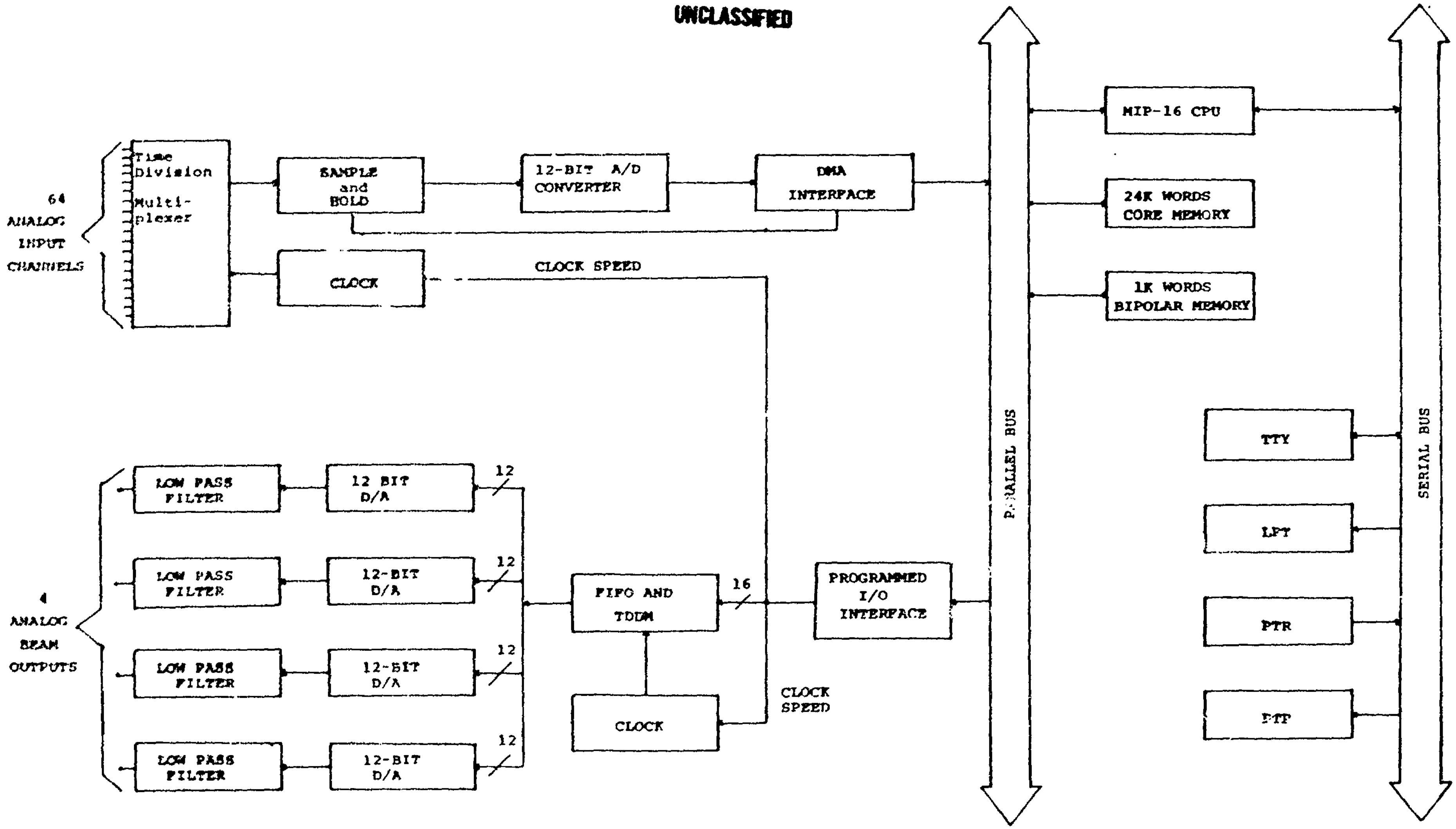

UNCLASSIFIED

FIGURE 2-4 SPRAY BEAMFORMER SYSTEM
BLOCK DIAGRAM

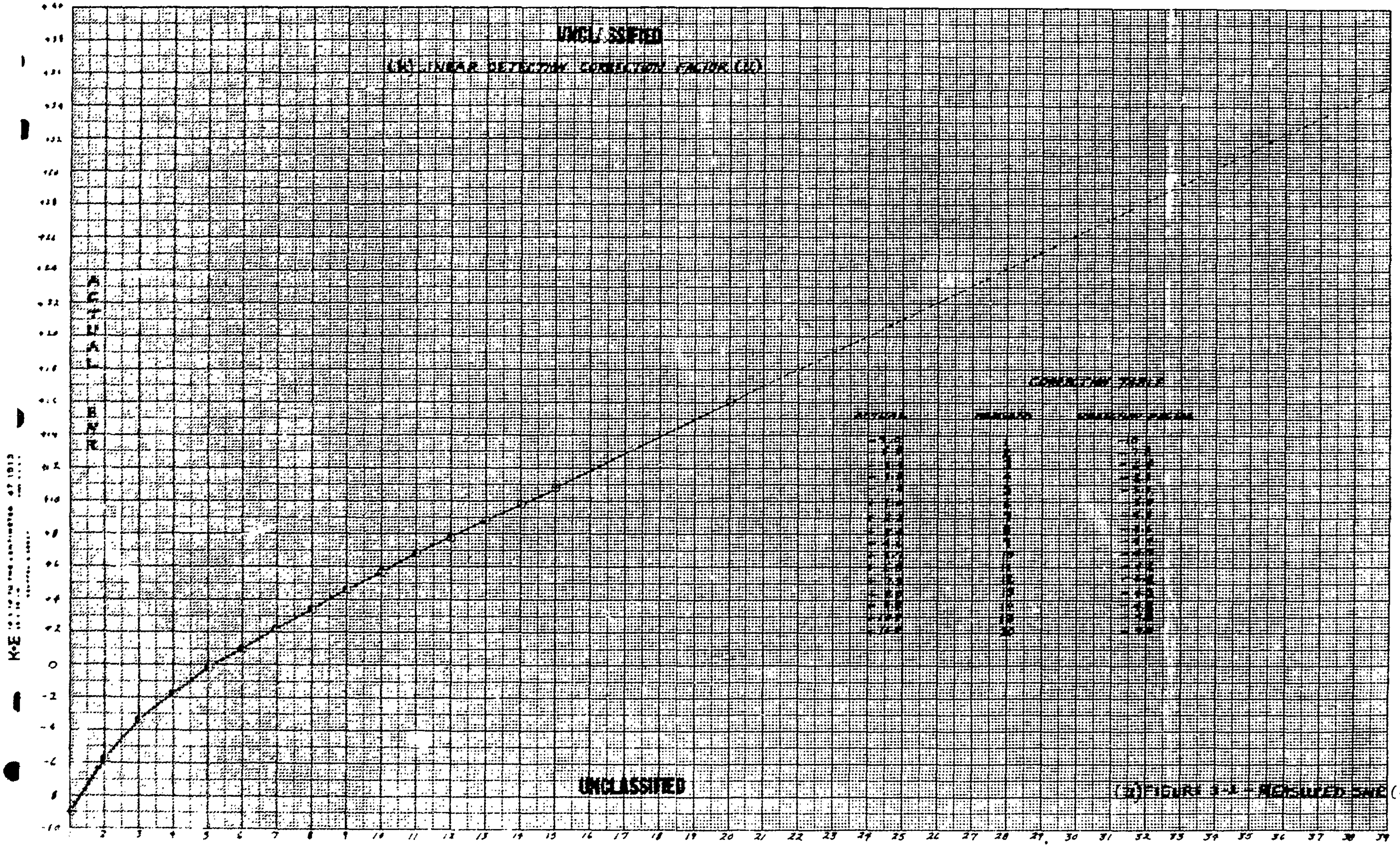

(U) FIGURE 3-4 - MEASURED SNR (U)

APPENDIX A

(U) SANDERS-DEVELOPED 6108 DIGITAL SIGNAL PROCESSOR SNR CALIBRATION RESULTS (U)

(U) These measurements in figures A-1 thru A-8, with a known signal level, verify that the displayed signal level is accurate to within 0.6 dB. (Some plots require two passes - one to obtain high signal level and the second pass to obtain accurate low noise levels).

(U) Sanders developed 4 channel beamformer calibration results.

(U) Figure A-9 is a plot of measured vs theoretical beamformed gain from a calibration tape. The plot displays a maximum error of 0.8 dBV. This calibration plot effectively checks the tape recorder and the beamformer. The data plotted in figure A-9 was obtained from the individual beamformed runs of figures A-10 thru A-15.

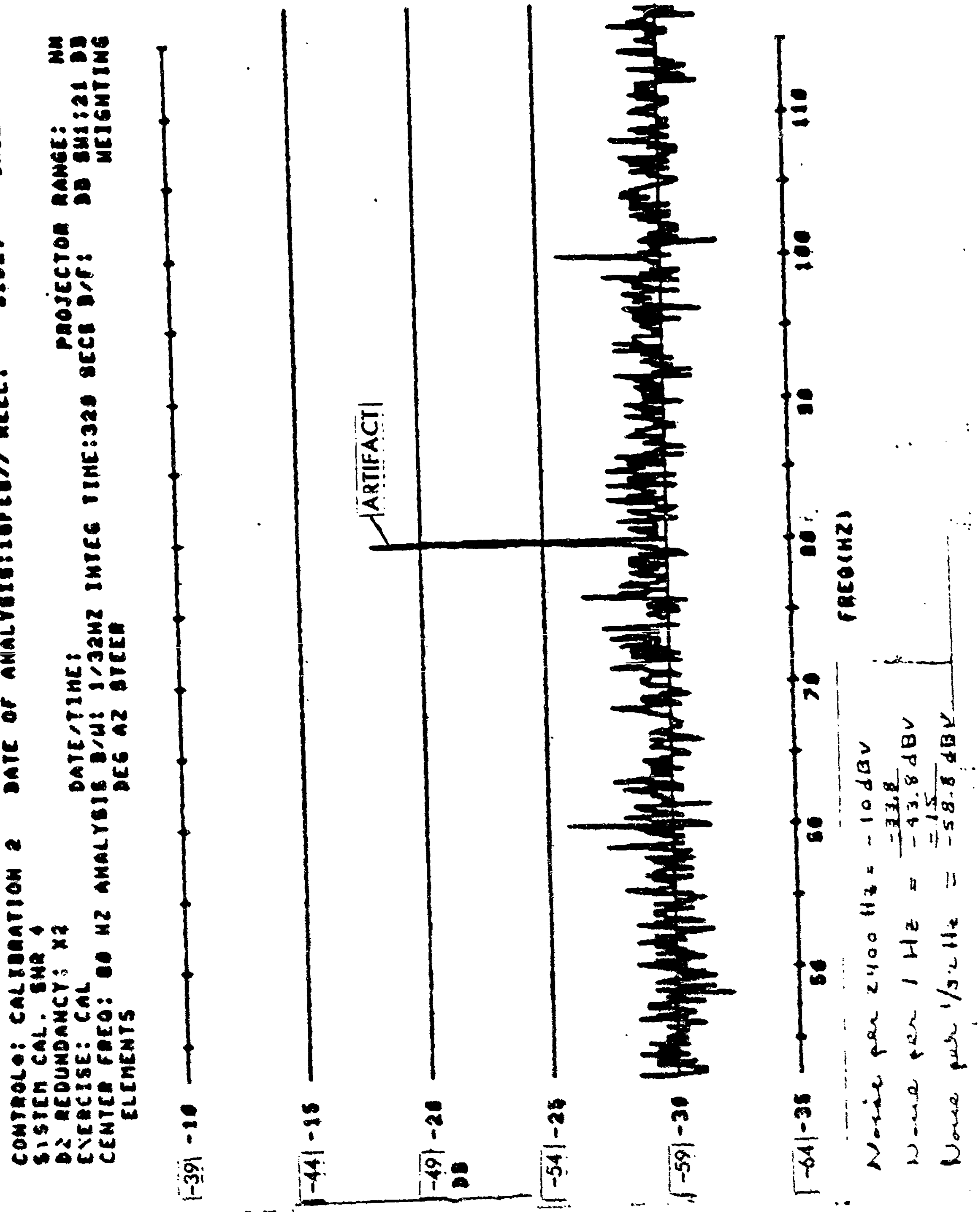

(U) Figure A-1 System Calibration at 100 Hz with -55 dBv Input. (U)

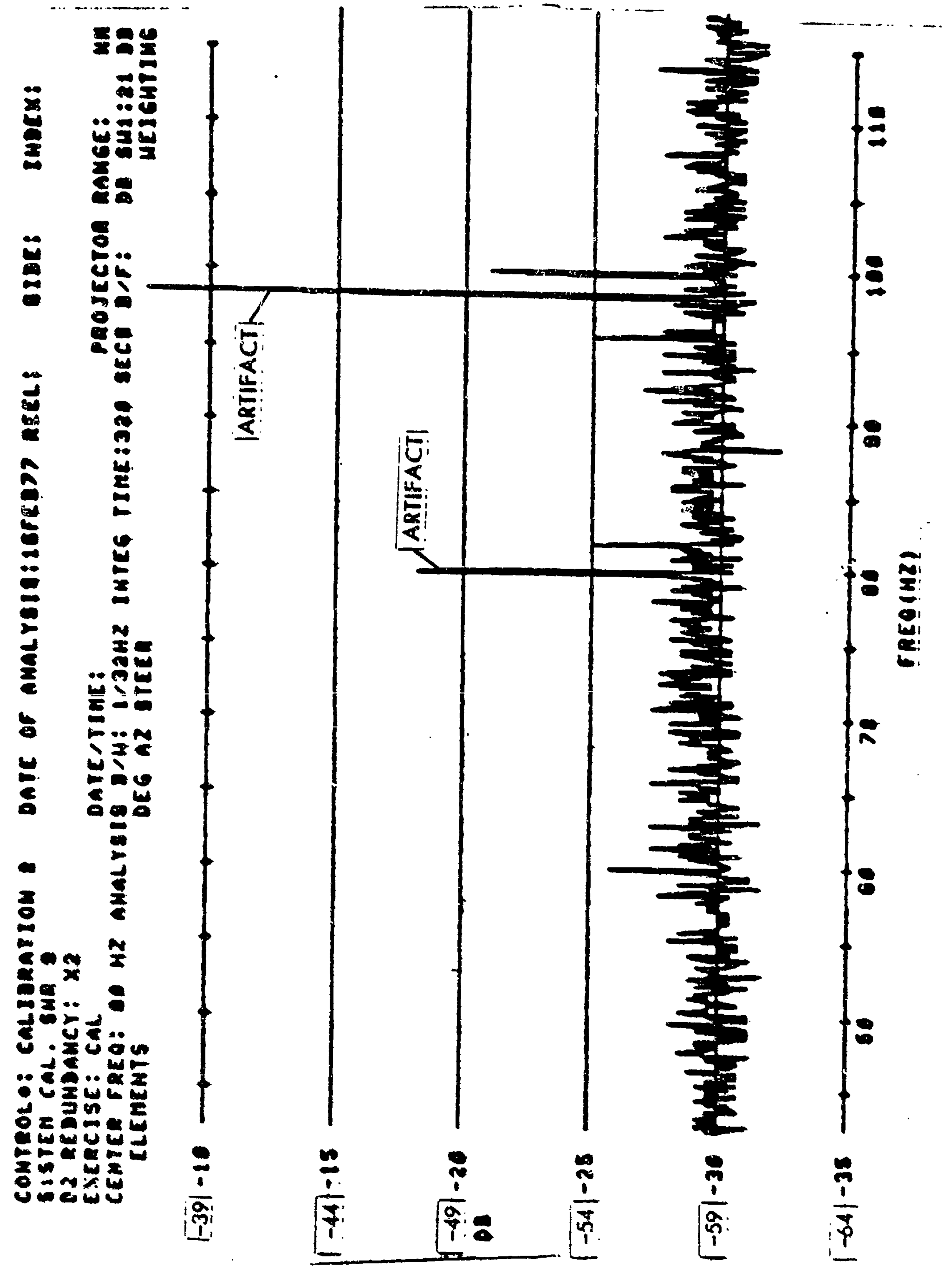

(U) Figure A-2 System Calibration at 100 Hz with -50 dBv Input. (U)

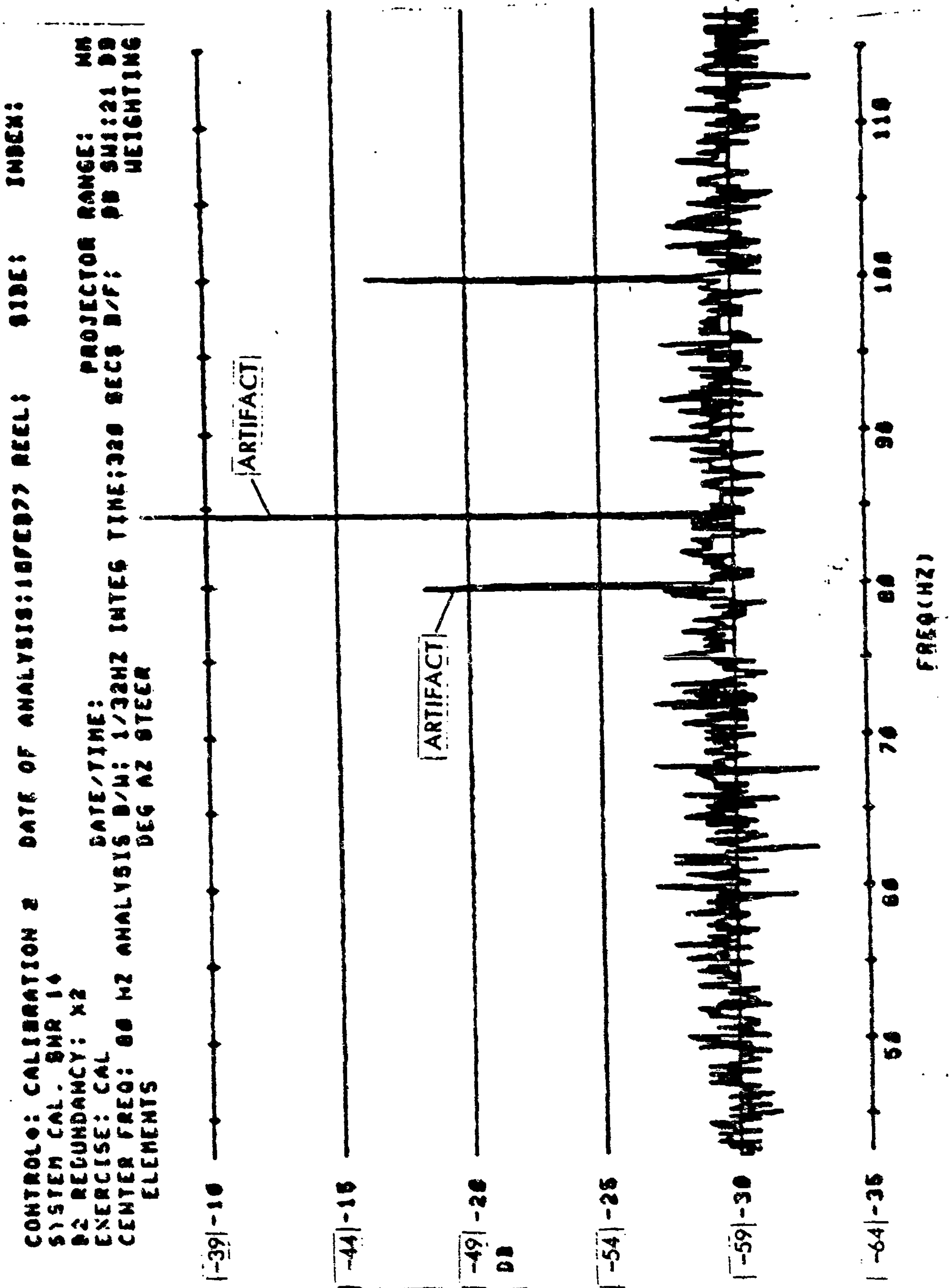

(U) Figure A-3 System Calibration at 100 Hz with -45 dBv Input. (U)

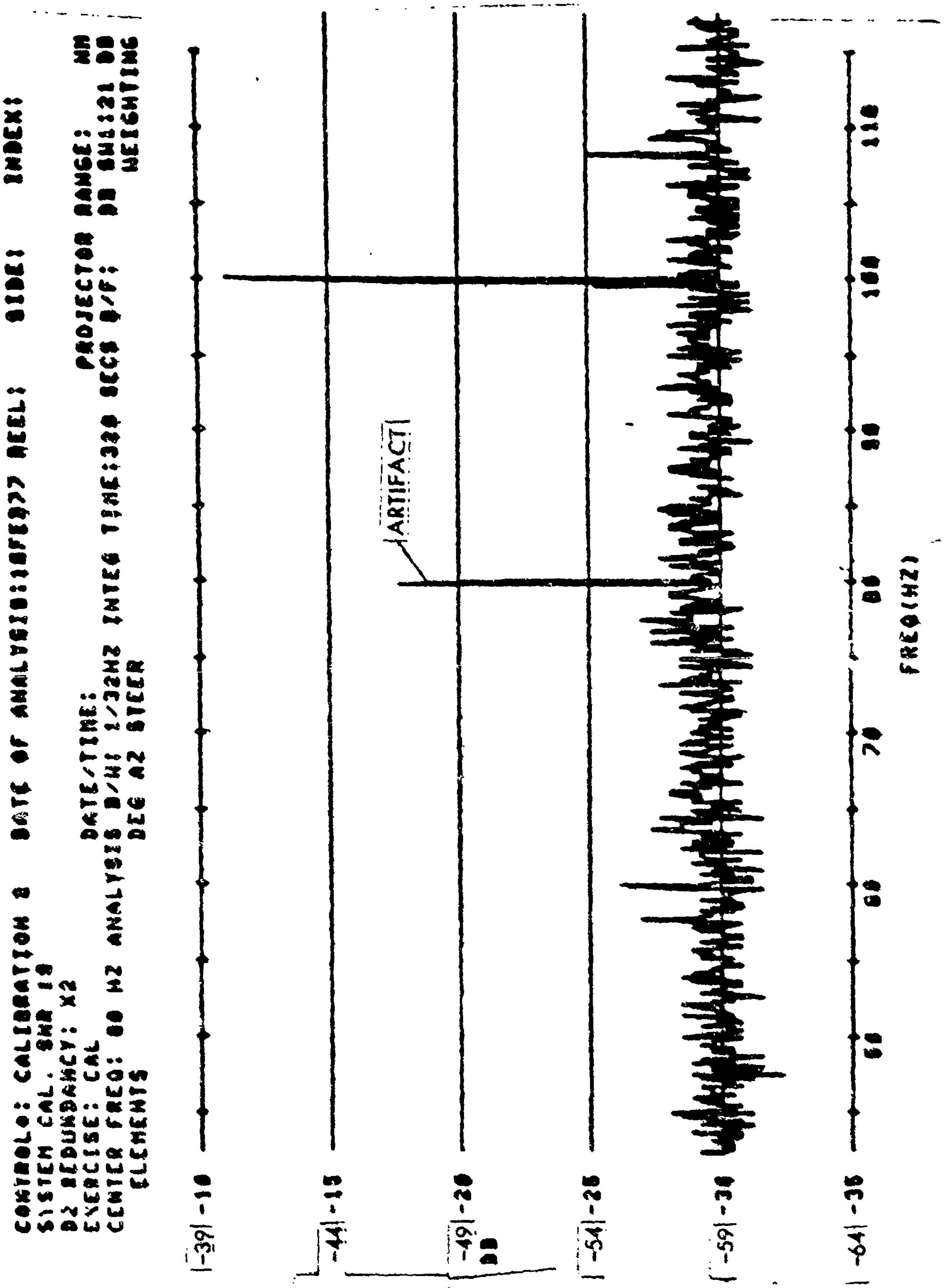

(U) Figure A-4 System Calibration at 100 Hz with -40 dBv Input.(U)

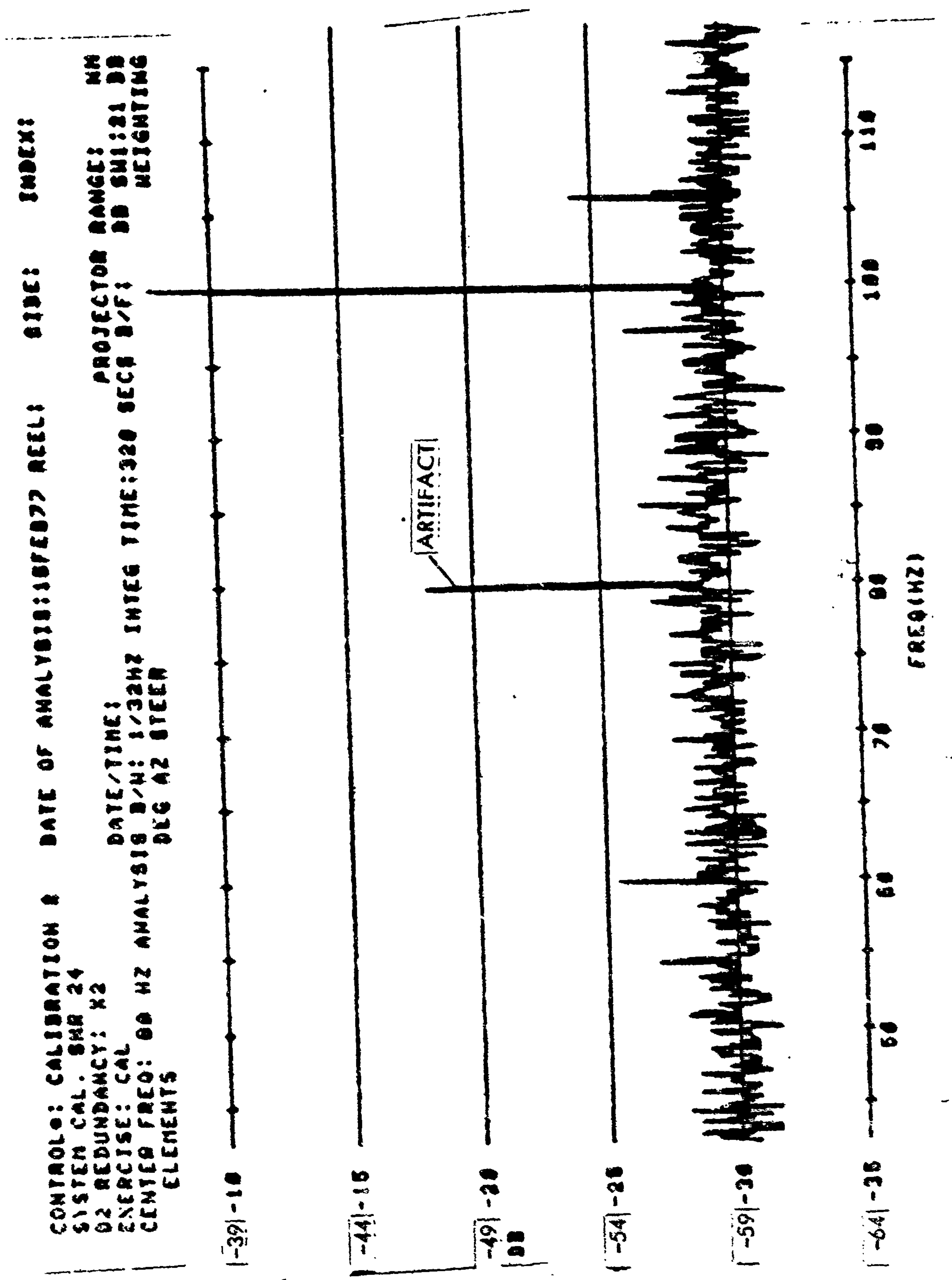

(U) Figure A-5 System Calibration at 100 Hz with -35 dBv Input (Sheet 1 of 2). (U)

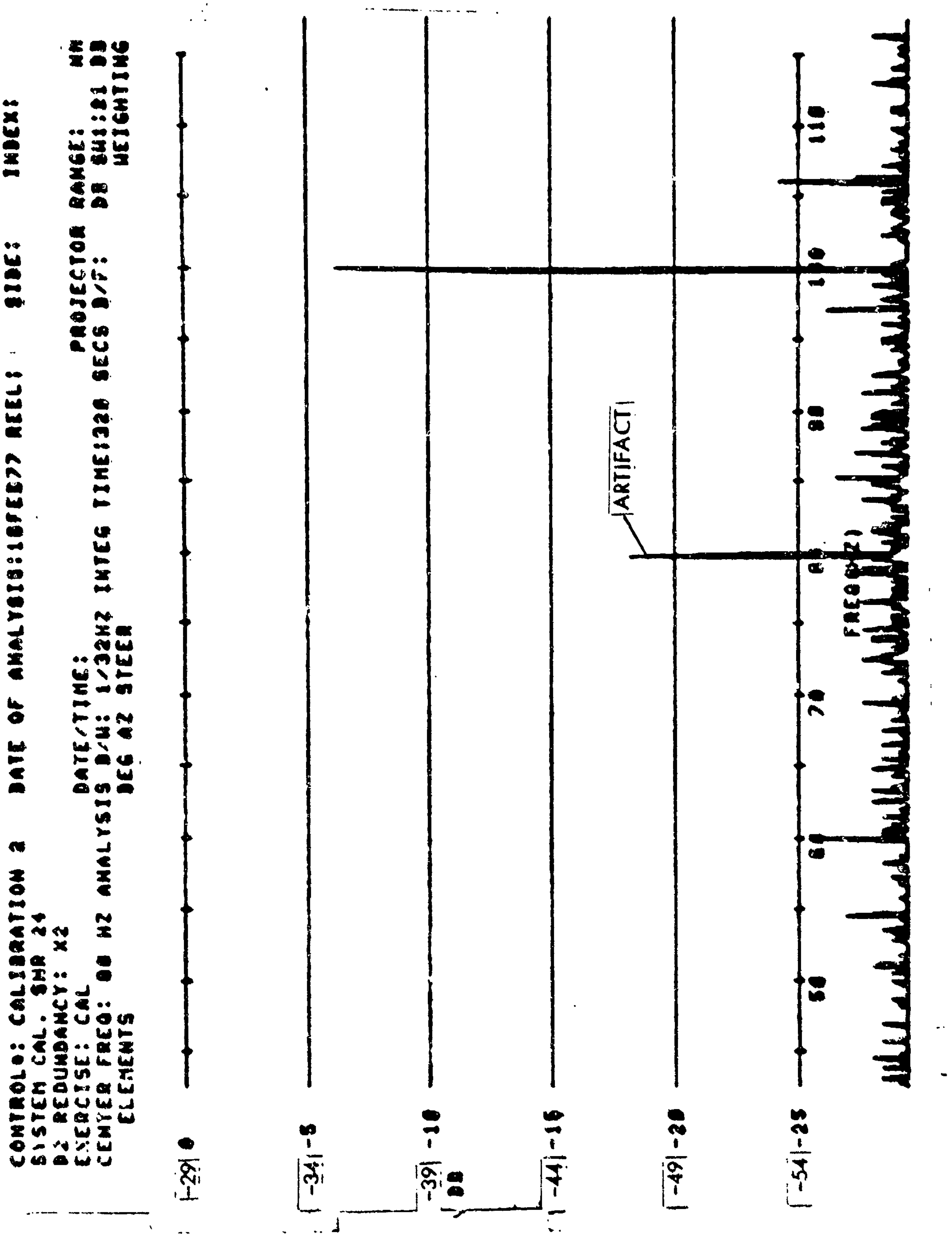

(U) Figure A-5 System Calibration at 100 Hz with -35 dBv Input (Sheet 2 of 2). (U)

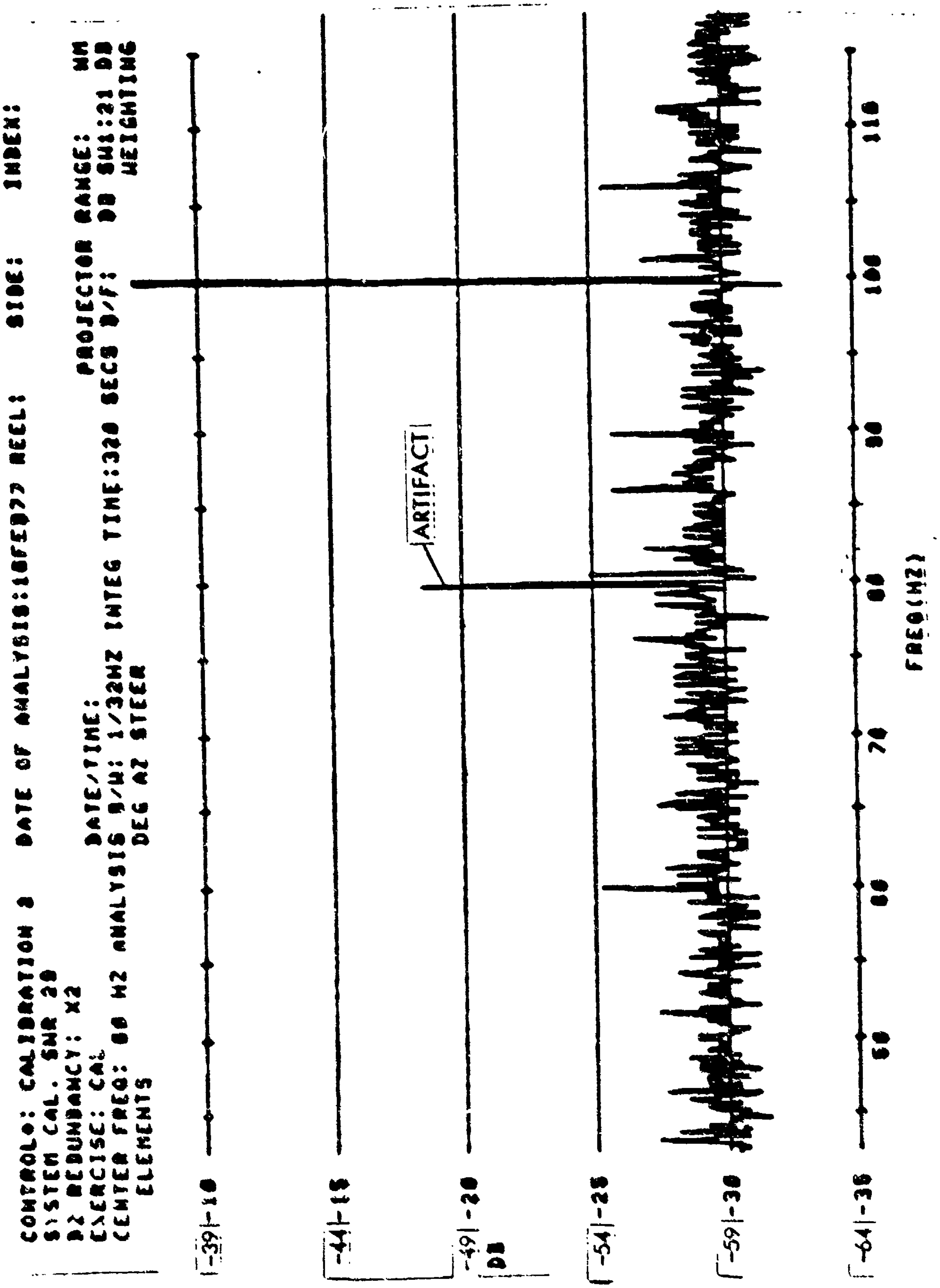

(U) Figure A-6 System Calibration at 100 Hz with -30 dBv Input (Sheet 1 of 2). (U)

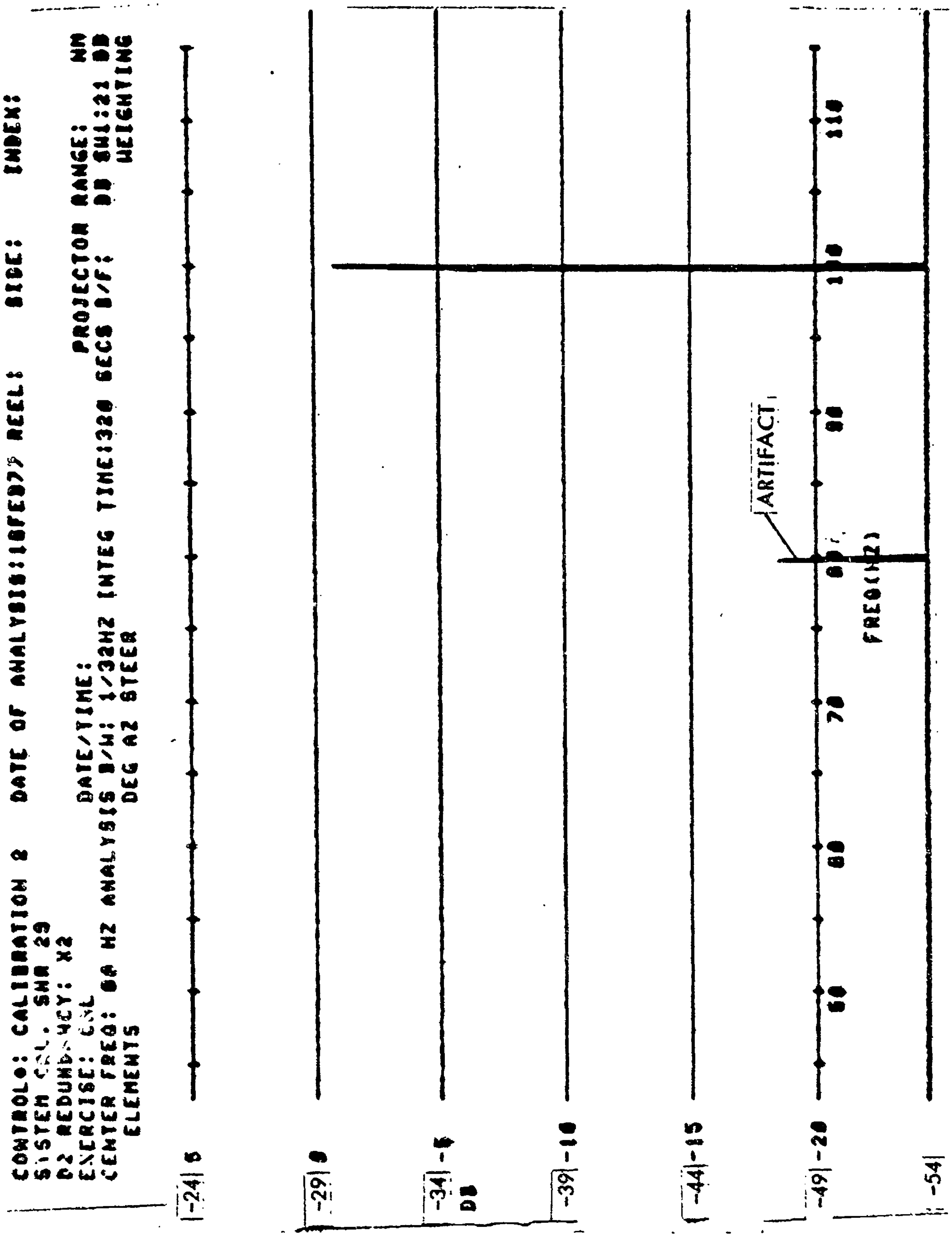

(U) Figure A-6 System Calibration at 10C Hz with -30 dBv Input (Sheet 2 of 2). (U)

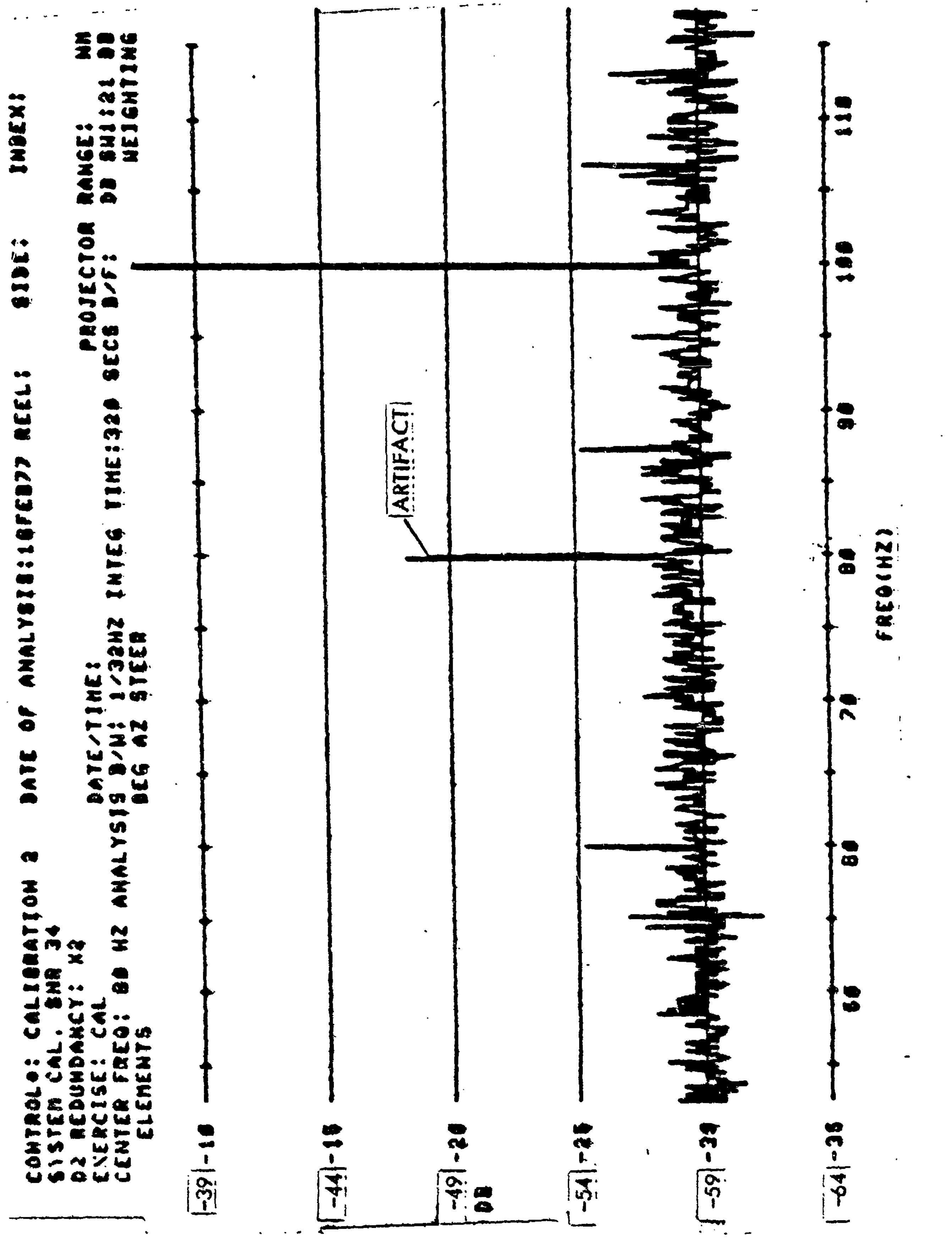

(U)Figure A-7 System Calibration at 100 Hz with -25 dBv Input (Sheet 1 of 2). (U)

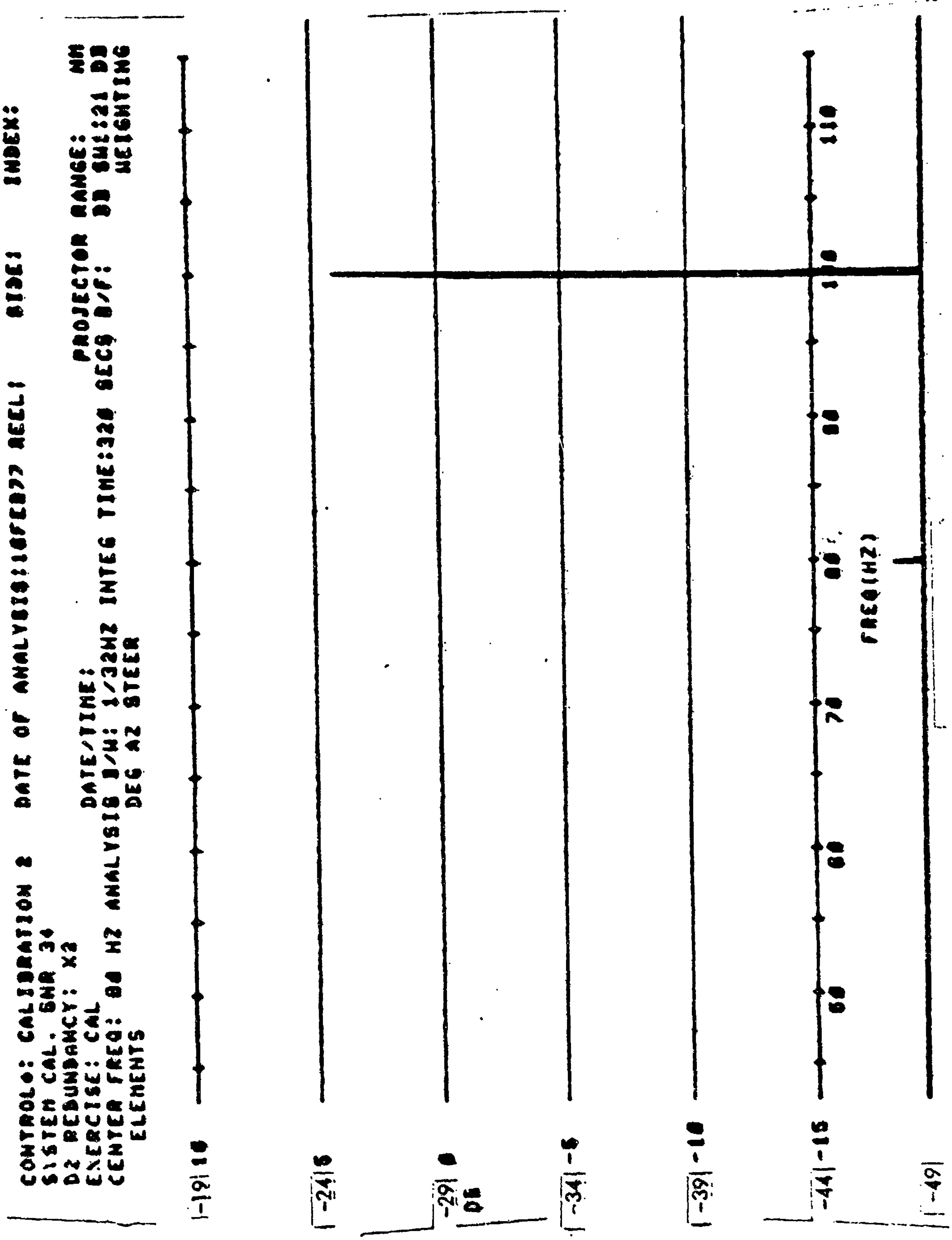

(U)Figure A-7 System Calibration at 100 Hz with -25 dBv Input (Sheet 2 of 2). (U)

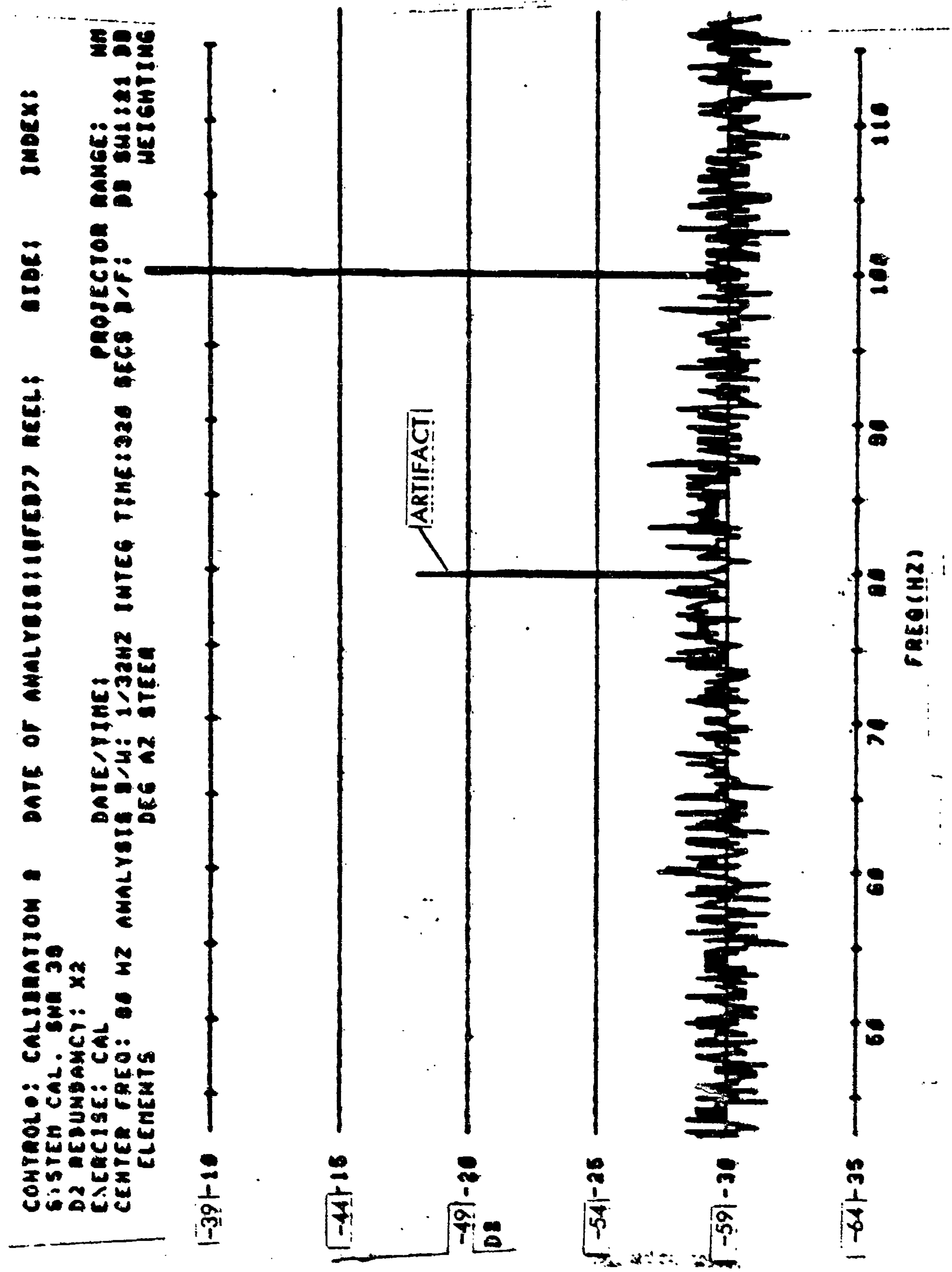

(U) Figure A-8 System Calibration at 100 Hz with -20 dBv Input (Sheet 1 of 2).(U)

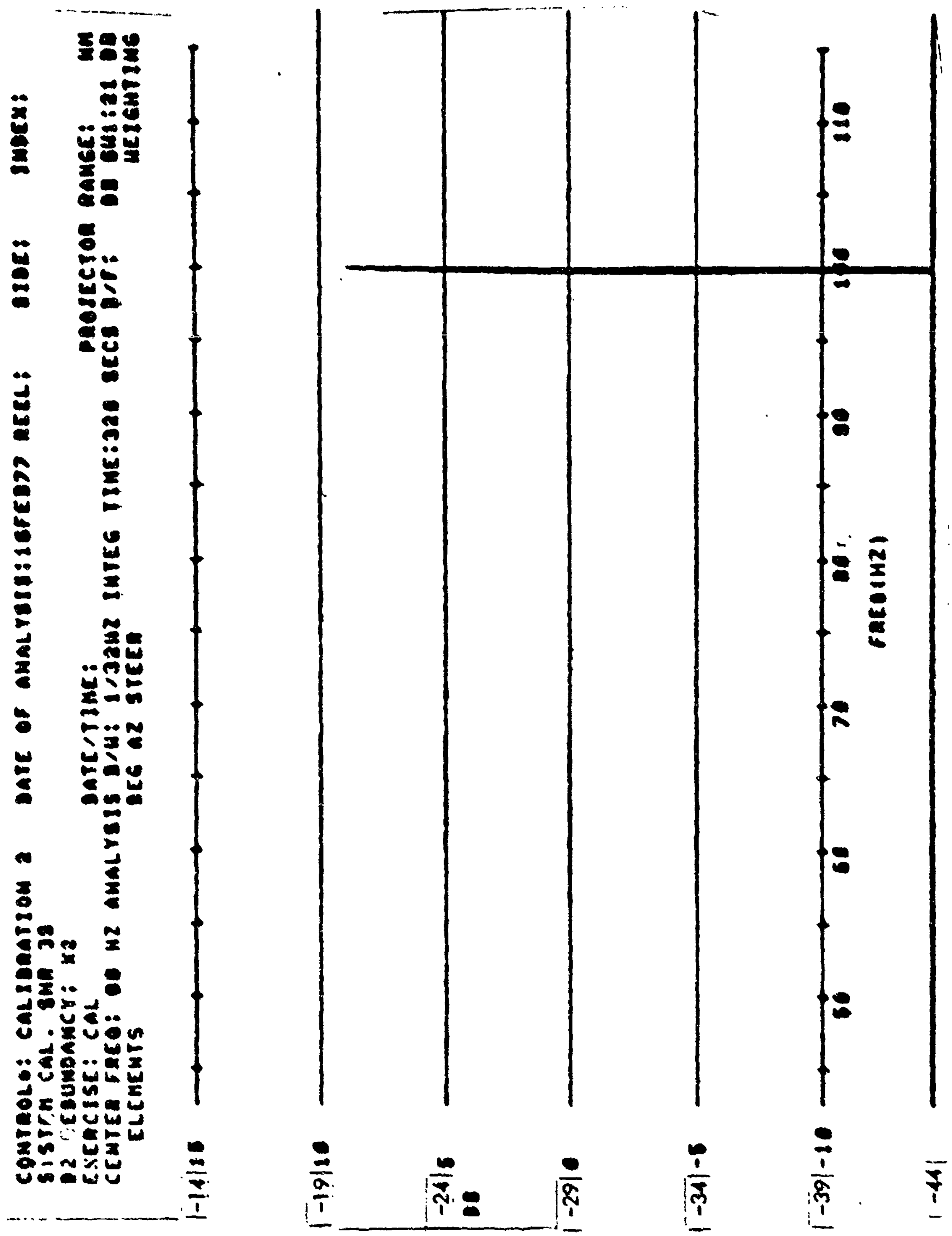

(U)Figure A-8 System Calibration at 100 Hz with -20 dBv Input (Sheet 2 of 2). (U)

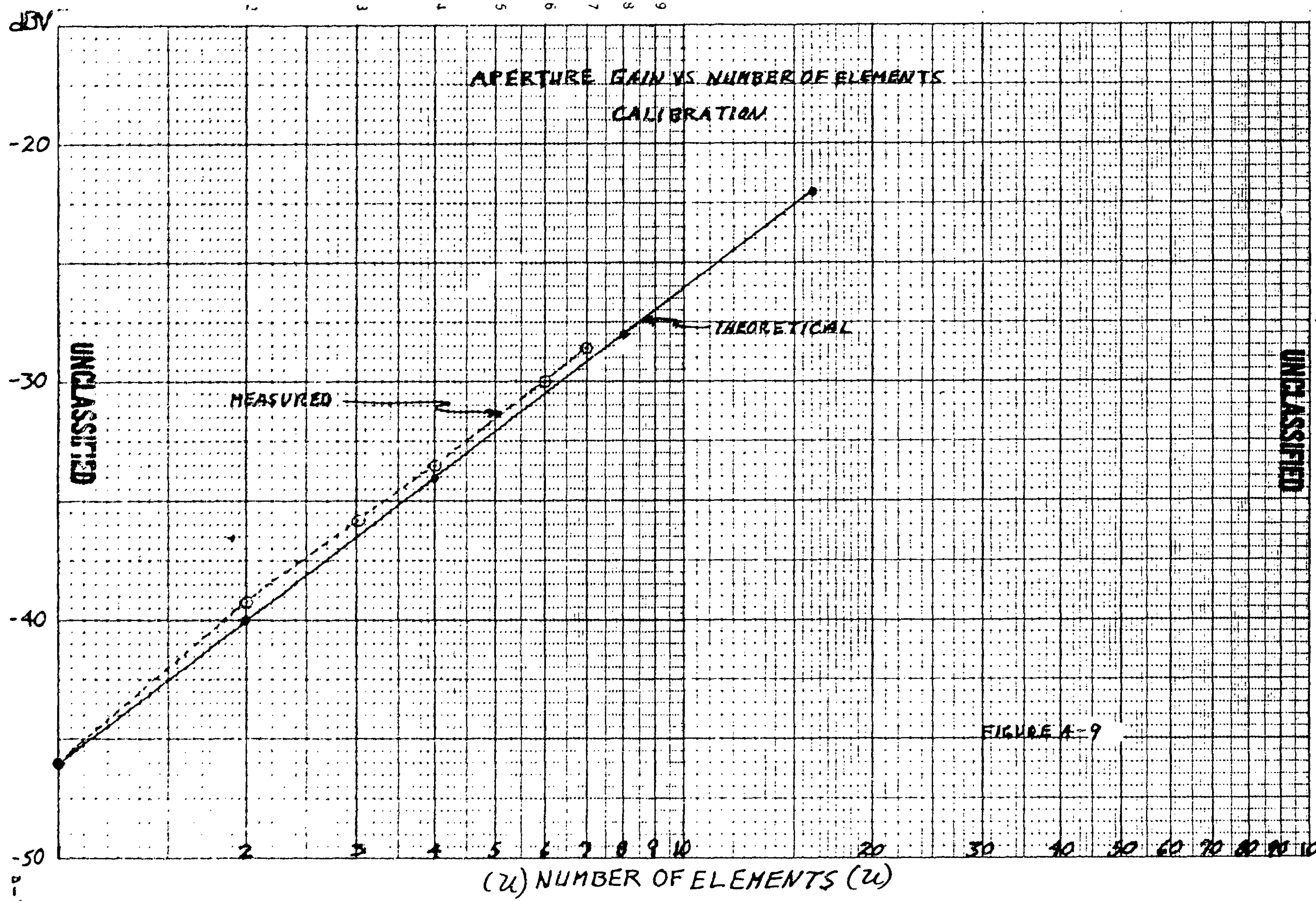

FIGURE A-9

UNCLASSIFIED

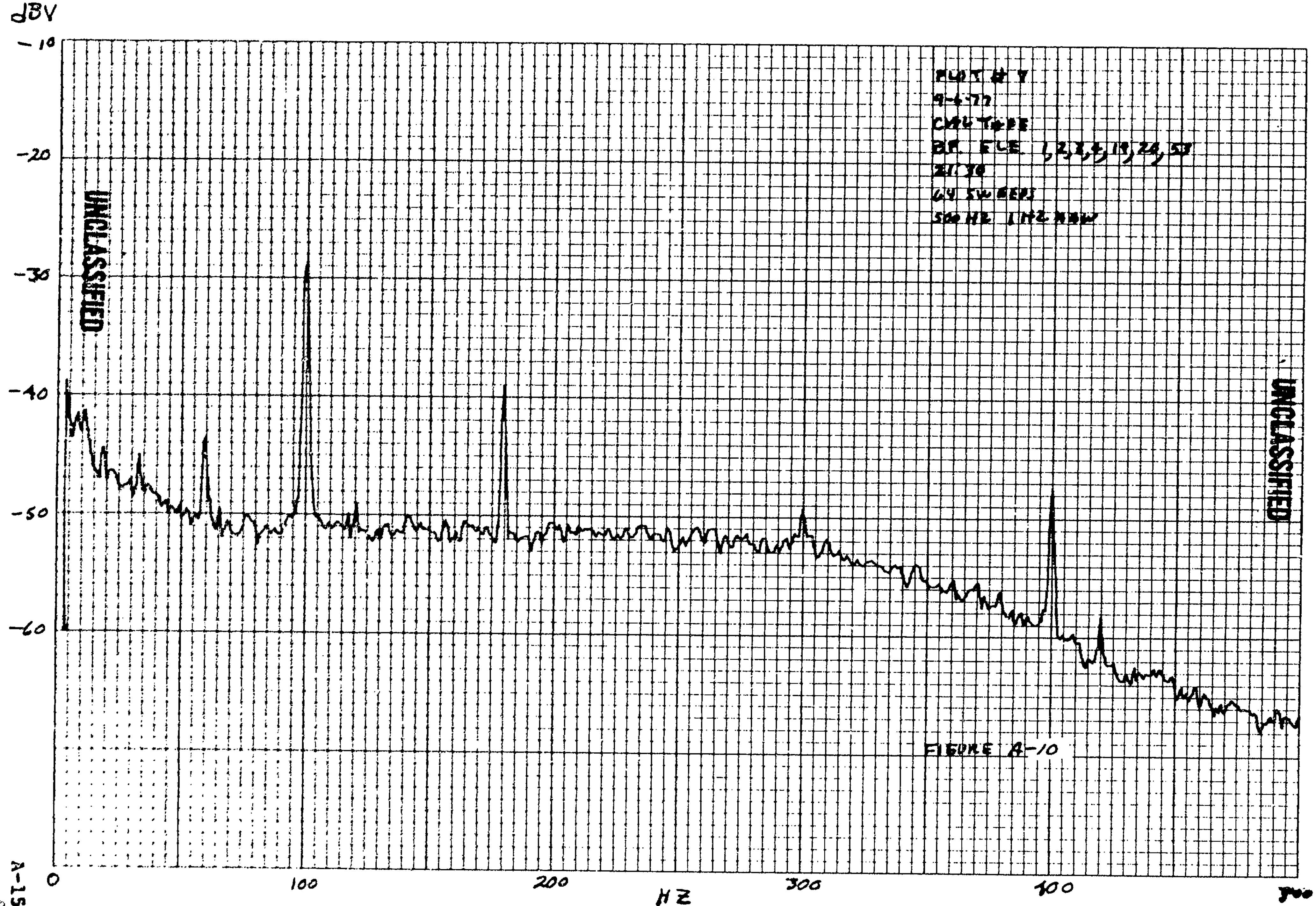

UNCLASSIFIED
dBV
-10
-20
-30
-40
-50
-60
0
100
200
300
400
500
HZ
9-6-77
64 SWEEPS
500 HZ
UNCLASSIFIED

FIGURE A-10

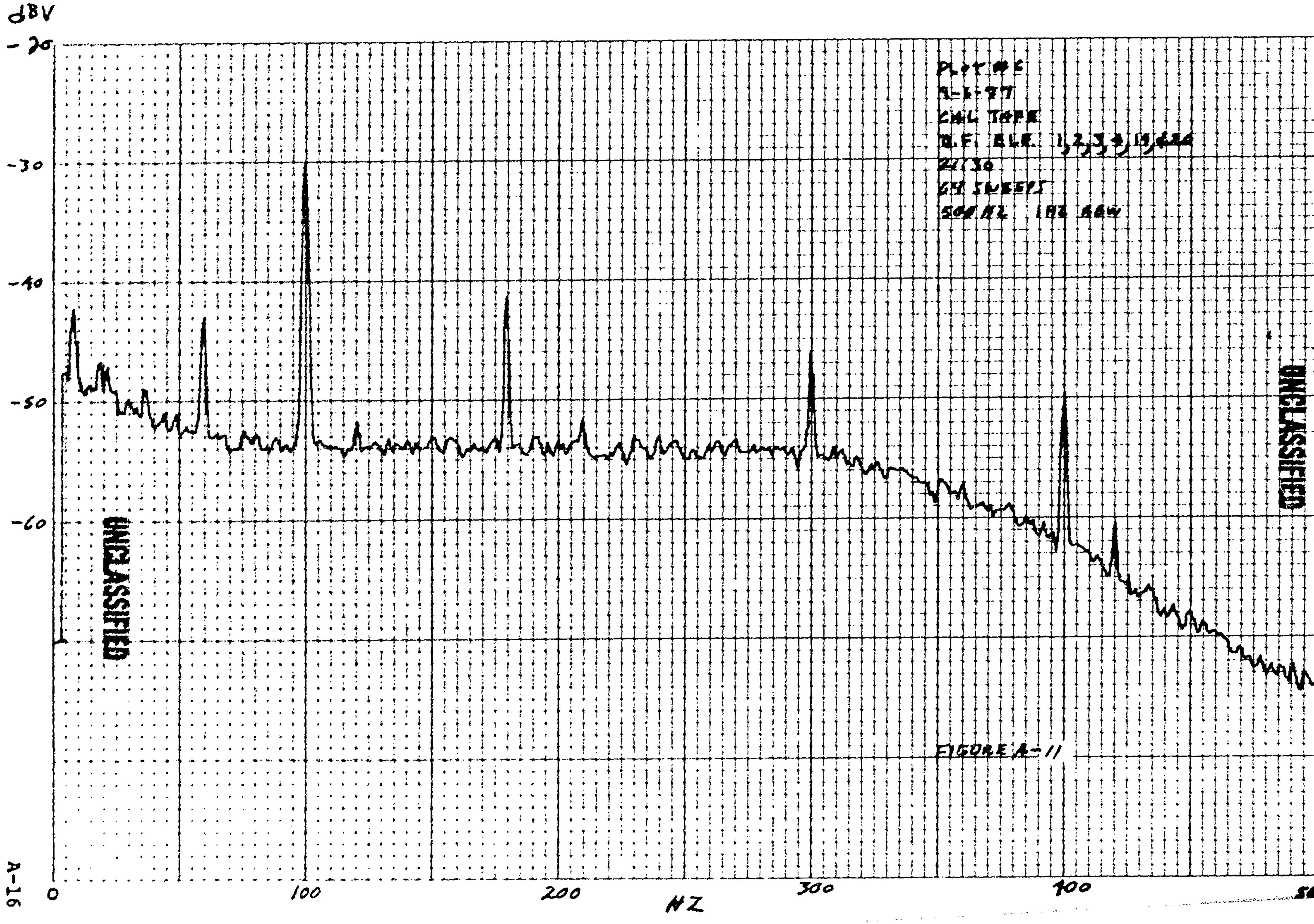

UNCLASSIFIED
dBV
-20
-30
-40
-50
-60
0
100
200
300
400
500
HZ
CAL TAPE
64 SWEEPS
500 HZ 1HZ BW
UNCLASSIFIED

FIGURE A-11

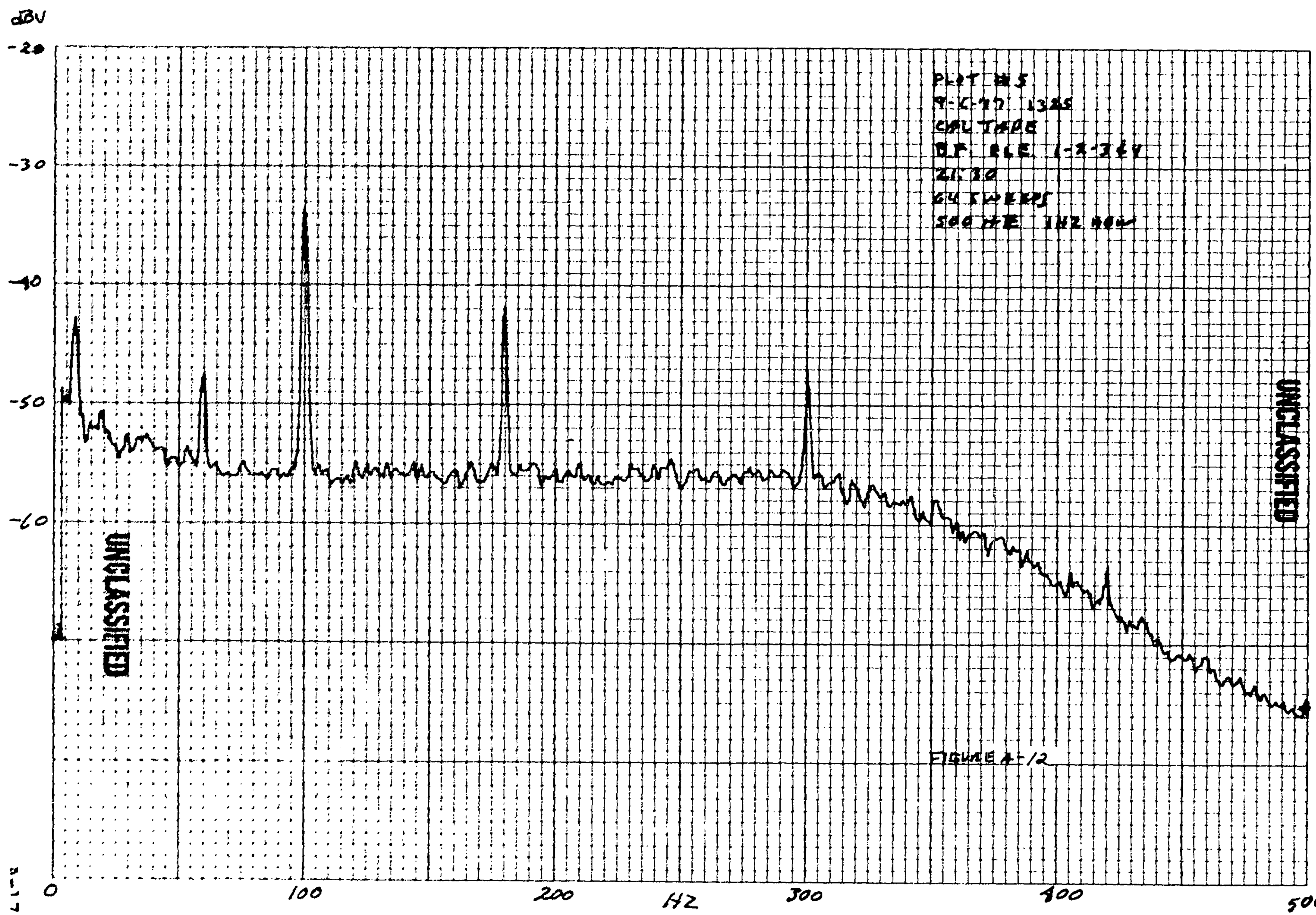
UNCLASSIFIED
dBV
-20
-30
-40
-50
-60
0
100
200
HZ
300
400
500
PLOT #5
9-6-77 1325
CAL TAPE
DF ELE 1-2-3-4V
21.30
64 SWEEPS
500 HZ 1HZ BW
UNCLASSIFIED

FIGURE A-12

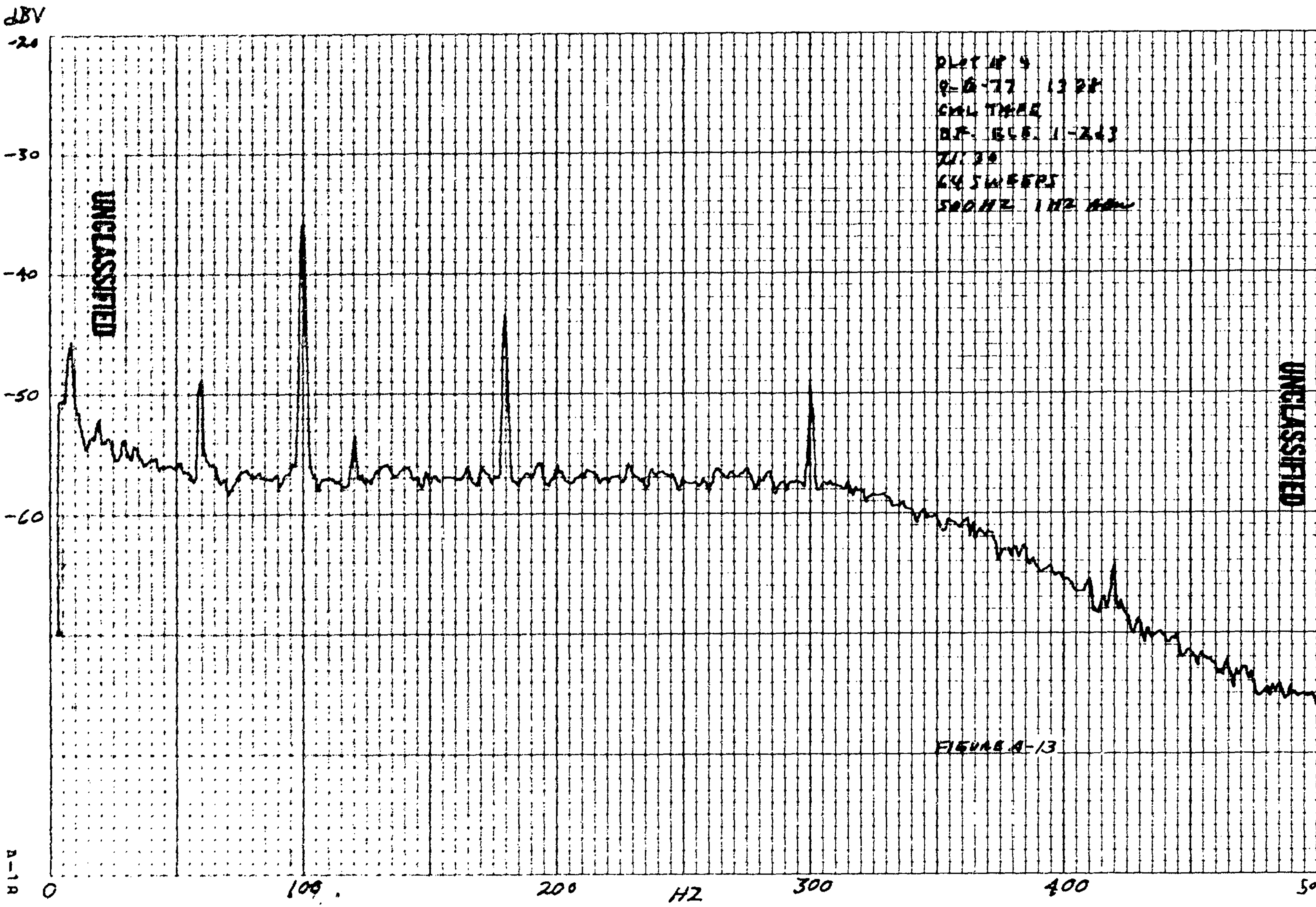

FIGURE A-13

03

UNCLASSIFIED

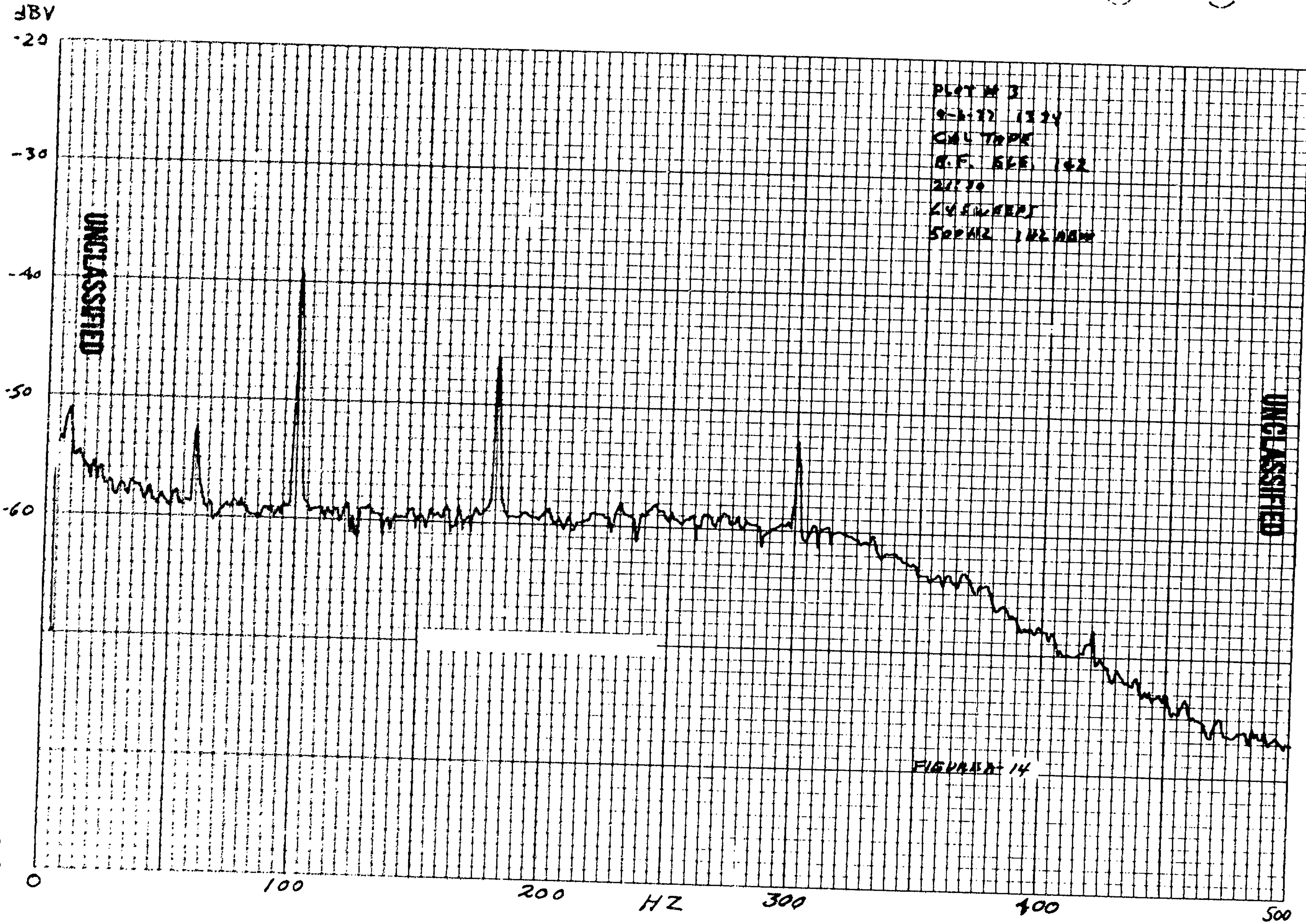

FIGURE A-14

UNCLASSIFIED

UNCLASSIFIED

703

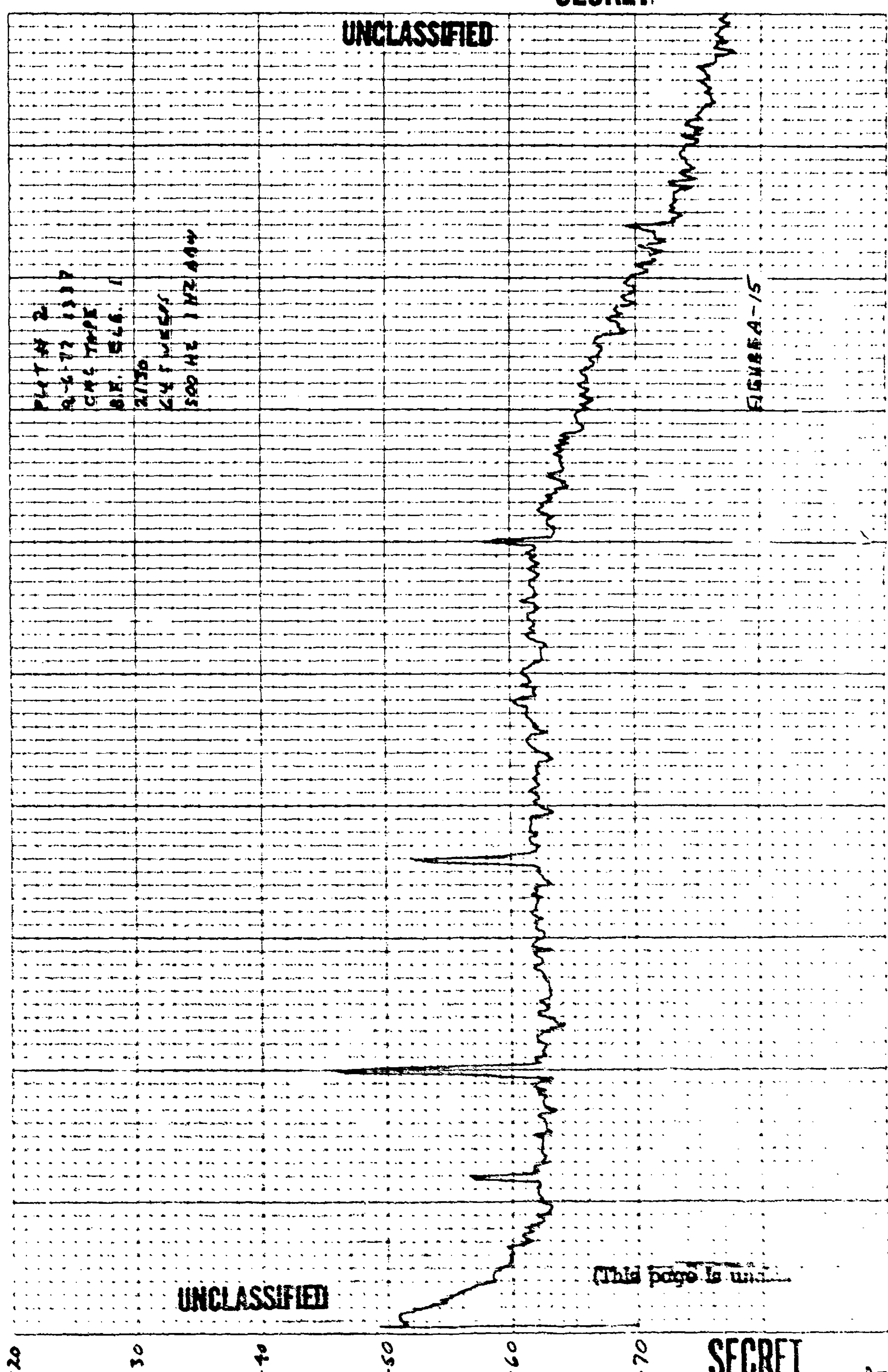

(This page is un

UNCLASSIFIED

SECRET

DEPARTMENT OF THE NAVY
OFFICE OF NAVAL RESEARCH
875 NORTH RANDOLPH STREET
SUITE 1425
ARLINGTON VA 22203-1995

IN REPLY REFER TO:

5510/1
Ser 321OA/011/06
31 Jan 06

MEMORANDUM FOR DISTRIBUTION LIST

Subj: DECLASSIFICATION OF LONG RANGE ACOUSTIC PROPAGATION PROJECT (LRAPP) DOCUMENTS

Ref: (a) SECNAVINST 5510.36

Encl: (1) List of DECLASSIFIED LRAPP Documents

1. In accordance with reference (a), a declassification review has been conducted on a number of classified LRAPP documents.

2. The LRAPP documents listed in enclosure (1) have been downgraded to UNCLASSIFIED and have been approved for public release. These documents should be remarked as follows:

   Classification changed to UNCLASSIFIED by authority of the Chief of Naval Operations (N772) letter N772A/6U875630, 20 January 2006.

   DISTRIBUTION STATEMENT A: Approved for Public Release; Distribution is unlimited.

3. Questions may be directed to the undersigned on (703) 696-4619, DSN 426-4619.

BRIAN LINK
By direction

Subj: DECLASSIFICATION OF LONG RANGE ACOUSTIC PROPAGATION PROJECT (LRAPP) DOCUMENTS

DISTRIBUTION LIST:

NAVOCEANO (Code N121LC – Jaime Ratliff)
NRL Washington (Code 5596.3 – Mary Templeman)
PEO LMW Det San Diego (PMS 181)
DTIC-OCQ (Larry Downing)
ARL, U of Texas
Blue Sea Corporation (Dr.Roy Gaul)
ONR 32B (CAPT Paul Stewart)
ONR 321OA (Dr. Ellen Livingston)
APL, U of Washington
APL, Johns Hopkins University
ARL, Penn State University
MPL of Scripps Institution of Oceanography
WHOI
NAVSEA
NAVAIR
NUWC
SAIC

Declassified LRAPP Documents

Report Number	Personal Author	Title	Publication Source (Originator)	Pub. Date	Current Availability	Class.
Unavailable	Bossard, David C.	ACOUSTIC ANALYSIS/ASEPS	Wagner Associates	780726	ADA076268	U
NRLMR3832	Heitmeyer, R., et al.	PRELIMINARY RESULTS OF AN ANALYSIS OF BEAM NOISE IN THE MEDITERRANEAN (U)	Naval Research Laboratory	780901	~~ND~~ ADC016220	U
Unavailable	Watrous, B. A.	PARKA 1 OCEANOGRAPHIC DATA COMPENDIUM	Naval Ocean R&D Activity	781101	ADB115967	U
Unavailable	Dunbar, B., et al.	LAMBDA PROCESSING LABORATORY AND ENGINEERING SUPPORT, FINAL REPORT 1 JANUARY 1977 - 31 OCTOBER 1978	Texas Instruments, Inc.	781129	ND	U
Unavailable	Blumen, L. S., et al.	ASTRAL MODEL. VOLUME 2: SOFTWARE IMPLEMENTATION	Science Applications, Inc.	790101	ADA956122	U
Unavailable	Spofford, C. W.	ASTRAL MODEL. VOLUME 1: TECHNICAL DESCRIPTION	Science Applications, Inc.	790101	ADA956124	U
Unavailable	Townsend, R., et al.	SELF-TENSIONING ACOUSTICAL HORIZONTAL LINE ARRAY (SPRAY) DATA ANALYSIS. FINAL REPORT OF BEARING STAKE TESTS JANUARY THRU MARCH 1977. VOLUME IA. OVERALL PROGRAM PERFORMANCE RESULTS WITH TEST RESULTS SUMMARY	Sanders Associates, Inc.	790101	ADC017573	U
Unavailable	Unavailable	SELF-TENSIONING ACOUSTICAL HORIZONTAL LINE ARRAY (SPRAY) DATA ANALYSIS. FINAL REPORT OF BEARING STAKE TESTS JANUARY THRU MARCH 1977. VOLUME IB. DETAILED DESCRIPTION, TEST RESULTS	Sanders Associates, Inc.	790101	ADC017574	U
Unavailable	Unavailable	SELF-TENSIONING ACOUSTICAL HORIZONTAL LINE ARRAY (SPRAY) DATA ANALYSIS. FINAL REPORT OF BEARING STAKE TESTS JANUARY THRU MARCH 1977. VOLUME II. DATA ANALYSIS FACILITY AND DATA REDUCTION METHODOLOGY	Sanders Associates, Inc.	790109	ADC017575	U
Unavailable	Unavailable	SELF-TENSIONING ACOUSTICAL HORIZONTAL LINE ARRAY (SPRAY) DATA ANALYSIS. FINAL REPORT OF BEARING STAKE TESTS JANUARY THRU MARCH 1977. VOLUME IIIA. DATA POINTS 1, 2 AND 3 RAW DATA	Sanders Associates, Inc.	790109	ADC017576	U
Unavailable	Unavailable	SELF-TENSIONING ACOUSTICAL HORIZONTAL LINE ARRAY (SPRAY) DATA ANALYSIS. FINAL REPORT OF BEARING STAKE TESTS JANUARY THRU MARCH 1977. VOLUME IIIB. DATA POINTS 4, 5 AND 6 RAW DATA	Sanders Associates, Inc.	790109	ADC017577	U
Unavailable	Unavailable	SELF-TENSIONING ACOUSTICAL HORIZONTAL LINE ARRAY (SPRAY) DATA ANALYSIS. FINAL REPORT OF BEARING STAKE TESTS JANUARY THRU MARCH 1977. VOLUME IVA. DATA POINTS 7, 8 AND 9 RAW DATA	Sanders Associates, Inc.	790109	ADC017578	U